Journal of Chemical Neuroanatomy 133 (2023) 102342

Contents lists available at ScienceDirect

Journal of Chemical Neuroanatomy

journal homepage: www.elsevier.com/locate/jchemneu

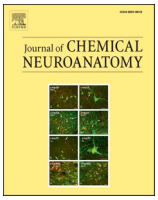

Activation patterns of dopaminergic cell populations reflect different learning scenarios in a cichlid fish, *Pseudotropheus zebra*

Calvo Roberta [a,*], Schluessel Vera [a], Hofmann Hans A [b], Hofmann Michael H [a]

[a] Institute of Zoology, Rheinische Friedrich-Wilhelms-Universität Bonn, Poppelsdorfer Schloss, Meckenheimer Allee 169, 53115 Bonn, Germany
[b] Department of Integrative Biology, Institute for Neuroscience, University of Texas at Austin, 2415 Speedway, Austin, TX 78712, USA

ARTICLE INFO

Keywords:
Brain
pS6
Dopamine
Behavior
Cichlid
Neural activation

ABSTRACT

Dopamine is present in all vertebrates and the functional roles of the subsystems are assumed to be similar. Whereas the effect of dopaminergic modulation is well investigated in different target systems, less is known about the factors that are causing the modulation of dopaminergic cells. Using the zebra mbuna, *Pseudotropheus zebra*, a cichlid fish from Lake Malawi as a model system, we investigated the activation of specific dopaminergic cell populations detected by double-labeling with TH and pS6 antibodies while the animals were solving different learning tasks. Specifically, we compared an intense avoidance learning situation, an instrumental learning task, and a non-learning isolated group and found strong activation of different dopaminergic cell populations. Preoptic-hypothalamic cell populations respond to the stress component in the avoidance task, and the forced movement/locomotion may be responsible for activation in the posterior tubercle. The instrumental learning task had little stress component, but the activation of the raphe superior in this group may be correlated with attention or arousal during the training sessions. At the same time, the weaker activation of the nucleus of the posterior commissure may be related to positive reward acting onto tectal circuits. Finally, we examined the co-activation patterns across all dopaminergic cell populations and recovered robust differences across experimental groups, largely driven by hypothalamic, posterior tubercle, and brain stem regions possibly encoding the valence and salience associated with stressful stimuli. Taken together, our results offer some insights into the different functions of the dopaminergic cell populations in the brain of a non-mammalian vertebrate in correlation with different behavioral conditions, extending our knowledge for a more comprehensive view of the mechanisms of dopaminergic modulation in vertebrates.

1. Introduction

The biogenic amine dopamine (DA) is a potent neuromodulator in all bilaterian animals (Wintle and Van Tol, 2001; Callier et al., 2003; Moroz et al., 2021) and plays a fundamental role in the regulation of approach and avoidance behaviors (O'Connell and Hofmann, 2011). In humans, dysregulation of the dopaminergic system underlies numerous neurological and psychiatric disorders [e.g. Parkinson's disease,

Abbreviations: ATN, anterior tuberal nucleus; *Cer*, cerebellum; *Dc*, central division of the dorsal telencephalon; *Dd*, dorsal division of the dorsal telencephalon; *Dl*, lateral division of the dorsal telencephalon; *Dld*, dorsal subdivision of the lateral division of the dorsal telencephalon; *Dlv*, ventral subdivision of the lateral division of the dorsal telencephalon; *Dmd*, dorsal subdivision of the medial division of the dorsal telencephalon; *Dmv*, ventral subdivision of the medial division of the dorsal telencephalon; *Dp*, posterior division of the dorsal telencephalon; *E*, entopeduncular nucleus; *fr*, fasciculus retroflexus; *Ha*, habenula; *Hc*, caudal hypothalamus; *Hyp*, hypothalamus; *IGL*, internal granular layer of the olfactory bulb; *IL*, inferior lobes of the hypothalamus; *ILr*, inferior lobe, nucleus of the lateral recess; *LC*, locus coeruleus; *NDI*, nucleus diffusus pars lateralis; *NG*, nucleus glomerulosus; *NLT*, nucleus lateralis tuberis; *nPR*, nucleus of the posterior recess; *nTP*, nucleus of the posterior tubercle; *OB*, olfactory bulb; *pc*, posterior commissure; *PP*, periventricular pretectal nucleus; *POAa*, preoptic area, anterior part; *POAp*, preoptic area, posterior part; *PTc*, pretectal area, centralis; *PTco*, pretectal area, corticalis; *pTP*, periventricular posterior tuberculum; *PTsm*, pretectal area, superficialis magnocellularis; *Ras*, raphe superior; *RFs*, superior reticular formation; *SCN*, suprachiasmatic nucleus; *SGN*, secondary gustatory nucleus; *Tel*, telencephalon; *TGN*, tertiary gustatory nucleus; *TL*, torus longitudinalis; *TLat*, torus lateralis; *TO*, tectum opticum; *Vc*, central nucleus of the ventral division of the telencephalon; *Vd*, dorsal nucleus of the ventral division of the telencephalon; *Vl*, lateral nucleus of the ventral division of the telencephalon; *VM*, ventromedial thalamic nucleus; *Vv*, ventral nucleus of the ventral division of the telencephalon.

* Corresponding author.
E-mail address: rcalvo@uni-bonn.de (C. Roberta).

https://doi.org/10.1016/j.jchemneu.2023.102342
Received 31 May 2023; Received in revised form 13 September 2023; Accepted 14 September 2023
Available online 16 September 2023

schizophrenia, attention deficit hyperactivity disorder (ADHD)] (Callier et al., 2003; O'Connell et al., 2011). Due to its critical role in regulating neural and behavioral processes, the dopaminergic system has therefore been studied in great detail, especially in mammals. The first evidence of the presence of dopamine-producing neurons came in the early 1960 s by Annica Dahlström and Kjell Fuxe, who also introduced the conventional numbering of the catecholaminergic cell populations from A1 to A12 in the rat brain (Dahlström and Fuxe, 1964). Later on, additional cell populations were added (A13 - A17) (Hökfelt, 1984; Lindvall and Björklund, 1984). This nomenclature of dopaminergic cell populations is still used today because dopaminergic cells are not located in a specific nucleus and furthermore their locations and distributions vary between vertebrates and even between different species of mammals (Yamamoto and Vernier, 2011). In general, dopaminergic cells (A8 to A17) are divided in different populations: retinal (A17), olfactory bulb (A16), diencephalic (A11–A15) and diencephalo-midbrain (A8–A10) populations (Smeets and González, 2000), while A1 to A7 cells are noradrenergic neurons localized in the medulla oblongata and pons (Nagatsu, 2007). In the central nervous system (CNS) of mammals, dopaminergic cell populations distribute their fibers in five major pathways (mesocortical, mesolimbic, nigrostriatal, tuberoinfundibular, and spinal tract systems). The mesocortical and mesolimbic pathways originate from the A10 neurons of the ventral tegmental area (VTA) and project respectively to the cortex and the nucleus accumbens (Horvitz, 2000; Wise, 2009). Together, they form the mesocorticolimbic system, which plays a central role in reward and motivation (Kelley and Berridge, 2002).

There is ample evidence that stressful and aversive stimuli can also result in dopamine release from the mesolimbic system (Ikemoto and Panksepp, 1999), suggesting the involvement of the dopaminergic system in the stress response (Salamone et al., 1997; Berridge and Robinson, 1998). The nigrostriatal pathway is involved both in learning and motor function and is formed by the A9 dopaminergic neurons in the substantia nigra projecting to the striatum (Hikosaka et al., 2002). Dopaminergic neurons from the arcuate and periventricular nuclei of the hypothalamus project to the pituitary gland, resulting in the tuberoinfundibular pathway, which is involved in the regulation of the secretion of prolactin from the pituitary (Demarest et al., 1984). Finally, the spinal projecting dopaminergic system originates from A10 and A11 cell populations (Qu et al., 2006). It is thought to modulate locomotion, but is also involved in sensory processing as it modulates nociception in the spinal cord (Piña-Leyva et al., 2022).

The dopaminergic system of non-mammalian vertebrates, especially that of teleost fishes, has received much less attention. Several studies have described dopaminergic neuron populations and, in some cases, fiber projections in a handful of species [e.g. goldfish *Carassius auratus* (Hornby et al., 1987), the brown ghost knifefish (*Apteronotus leptorhynchus*; Sas et al., 1990), the zebrafish (*Danio rerio*; Rink and Wullimann, 2001; Kaslin and Panula, 2001), and Burton's mouthbrooder cichlid (*Astatotilapia burtoni*, O'Connell et al., 2011; O'Connell et al., 2013a)]. Although some differences exist to the situation in mammals, there is broad consensus that the major dopaminergic components found in mammals are conserved in teleosts. However, to which extent the teleost dopaminergic system is functionally similar to its mammalian counterpart is much less clear.

DA plays an important role in learning in many vertebrates. Many areas in the telencephalon are rich of dopamine receptors like the striatum, amygdala, and hippocampus and their involvement in learning is well established (El-Ghundi et al., 2007; Puig et al., 2014). There is also evidence for the role of DA in learning in motor and sensory areas (Macedo-Lima and Remage-Healey, 2021). Although homologies of telencephalic areas between mammals and teleosts are uncertain, DA seems to play a role in learning also in fishes (e.g. Naderi et al., 2016).

Several studies have assessed the activation of different brain areas during different behavioral contexts using neural marker (i.e. immediate early genes – IEGs – for a review see Calvo and Schluessel, 2021). To get a more detailed understanding of the function of the dopaminergic system in teleost, the IEGs have been used to selectively mark the activation of dopaminergic cell populations. O'Connell et al., (2013b) investigated whether social stimuli would induce c-fos expression in dopaminergic populations in the brain of *A. burtoni*. They observed an increase of c-fos in the Vc of both intruder and reproductive opportunity contexts compared to the control group (O'Connell et al., 2013b). The same animal model was used by Weitekamp and Hofmann (2017) to assess whether cooperation would increase the activity of specific dopaminergic cell populations (Weitekamp and Hofmann, 2017). In larvae of zebrafish, handling stress, chemical stressor and pH change were reported to induce c-fos expression in the dopaminergic cell populations of the posterior tuberculum and hypothalamus (Semenova et al., 2014) and olfactory deprivation has an effect of the dopamine system within the olfactory bulb (Kress and Wullimann, 2012). These studies focused on specific dopaminergic subsystems.

Whereas zebrafish offer several advantages to study basic functions of the nervous system, other fish groups have also been subjects of different behavioral and anatomical studies. Cichlids are well studied and the organization of their brains and their complex behavior well documented (e.g. Pollen et al., 2007; Shumway, 2008, 2010). The distribution of tyrosine hydroxylase positive (TH+) cell populations and dopaminergic receptors has been investigated in detail (O'Connell et al., 2011). In addition, activity markers have been applied to study the activation of many different brain areas during different learning situations (Calvo et al., 2023).

In the present study, we examined the activation of the dopaminergic systems in the zebra mbuna cichlid, *P. zebra,* by co-labeling TH with the phosphorylated ribosome marker pS6, now commonly used to visualize neural activation in fish (Calvo et al., 2023 and references therein). In particular, we investigated the activation of thirteen different dopaminergic cell populations in fish subjected to two learning tasks that differed in the level of stress, locomotion, motivation, and reward. We hypothesized that different behavioral components would activate different dopaminergic populations.

2. Material and methods

2.1. Behavioral experiments

Animals used in this study (N = 30) were zebra mbuna cichlids, *Pseudotropheus zebra*, from the east African Lake Malawi. Fish were obtained from a commercial aquarist shop and were between 4.0 cm and 11.0 cm in total length. All individuals were maintained in captivity and sex could not be determined phenotypically. The same individuals were assessed in a previous study concerning activation of different brain areas by investigating the activity of the ribosomal marker pS6 (Calvo et al., 2023). For a detailed explanation of the experimental procedures and setups, we refer the reader to Calvo et al., 2023. Briefly, fish were kept in isolation for one week prior to being stressed (Avoidance group), trained (Trained group) and/or killed (Isolation group). Fish were housed in aerated and filtered 50-L aquaria (62 cm × 31 cm × 31 cm) at a temperature of 25–26 °C. Fish in the Isolation group (N = 10) did not receive any treatment and were killed after seven days of isolation. Fish in the Avoidance group (N = 10) were moved to a new smaller tank (31 cm × 15 cm x 15 cm) after seven days of isolation and chased with a net for one hour to simulate a strong stressor. Fish were killed 90 min after the chase ended. Fish in the Trained group (N = 10) underwent a daily visual training after seven days of isolation. During the training, the fish had to make a choice between the two different training symbols [a black dot over a white background (positive stimulus) and a white background without a symbol (alternative, negative stimulus)] projected onto the plexiglass of the experimental tank (see Schluessel et al., 2018 for details of the experimental setup). A correct choice was rewarded with food. After the learning criterion was achieved (seven or more correct decisions out of ten trials in three consecutive sessions), fish went through a so called "supersession" (1-hour non-stop training).

Then, the fish were killed 90 min after the supersession was finished. To process the brains, fish were anesthetized with tricaine methanesulfonate (MS-222). The spinal cord was transected and the brain was removed and fixed overnight in 4% paraformaldehyde (PFA) at 4 °C, then cryo-protected overnight in 30% sucrose at 4 °C. The following day, the brains were embedded in O.C.T compound (freezing medium, Leica Biosystem Richmond) and frozen at − 20 °C. Thirtyfive μm thick sections were cut at − 20 °C with a cryostat (Leica CM1520) and collected in three series on slides. One series was used for tyrosine hydroxylase immunohistochemistry (IHC) alone, one series for double-labeling with TH and pS6 antibodies and one series for cresyl violet staining for a cytoarchitecture reference. To minimize differences in stain intensity, IHC was performed twice within three days, each time including five brain per group (i.e. 5 control, 5 avoidance, 5 trained), starting from the day after the cutting.

2.2. Immunohistochemistry for tyrosine hydroxylase

Immunohistochemistry was performed as described previously (Calvo et al., 2023). Briefly, frozen sections were bleached in 1% H_2O_2 in phosphate-buffered saline (PBS), 0.01 M, pH 7.4, washed, and blocked in 10% normal goat serum (NGS) for 1 h then transferred to a primary antibody solution [5% NGS / 1X PBS - 0.3% Triton X-100, rabbit anti-tyrosine hydroxylase antibody - Neuronal Marker ab112 (abcam, Cambridge MA): 1:500] overnight at 4 °C, before being washed several times in PBS. The second antibody reaction (VECTASTAIN biotinylated anti-rabbit IgG secondary antibody, Vector Labs., USA: 1:500) was performed in 5% NGS / 1X PBS - 0.3% Triton X-100, followed by repeated washes in PBS. Then, signal amplification was initiated using the ABC method (1:1500, 1X PBS - 0.3% Triton X-100, VECTASTAIN ABC-Peroxidase kit, Vector Labs., USA) and visualized using the chromogen-solution [one 3,3'-Diaminobenzidine-Tetrahydrochloride (DAB) buffer tablet (Merck KGaA, Germany) dissolved in 15 ml distilled water, 500 μL 1% ammonium nickel sulphate, 12 μL 30% H_2O_2] for ~30 min. Sections were then dehydrated in ascending alcohols to xylene before cover slipping with Eukitt (Carl Roth, Germany).

2.3. Fluorescent co-labeling of pS6 and TH

To quantify the activation of dopaminergic neurons, pS6 and TH were co-localized by fluorescent double-labeling immunohistochemistry using a mix of 1:500 rabbit anti-tyrosine hydroxylase antibody (Neuronal Marker ab112 abcam, Cambridge MA) and 1:500 mouse anti-pS6 (Ser235/236 antibody, Cell Signaling E2R1O). To our knowledge, there are no published reports on the mouse anti-pS6 antibody used in this study. A rabbit anti-pS6 antibody from Cell Signaling ((Ser235/236) antibody, Cell Signaling 2211 S) has been used successfully in several studies on fish, including cichlids (for references see Calvo et al., 2023). Dr. Ross DeAngelis, from Hans Hofmann's laboratory group in Austin (Texas, United States), performed a double-labeling rabbit anti-pS6 and mouse anti-pS6 in the cichlid *Astatotilapia burtoni* showing no differences in the staining, that is rabbit anti-pS6 and mouse anti-pS6 stained the exact same cells (results not shown here). After incubation overnight in primary antibody, slides were washed twice in PBS and then incubated in a mix of 1:500 goat anti-rabbit IgG (H+L) cross-absorbed secondary antibody Alexa Fluor 594 and 1:500 goat anti-mouse IgG (H+L) cross adsorbed secondary antibody Alexa Fluor 488 (ThermoFisher scientific, Dallas, Texas, United States). Slides were then rinsed twice in PBS and cover-slipped with 4', 6-diamidino-2-phenylindole (DAPI) hardset fluorescent mounting media (Vector Laboratories, Burlingame, CA, USA).

The anti-tyrosine hydroxylase antibody was the same as in the single DAB immunohistochemistry protocol. The staining pattern in the double-labeling and single-labeling material was identical. Furthermore, the staining was very similar to the one reported by O'Connell et al. (2011). They noted that their antibody recognized both forms of TH (TH1 and TH2), but with a weaker staining of TH2.

2.4. Cell count

Thirteen dopaminergic cell populations were analyzed in each individual. The locations of the cell populations throughout the cichlid brain are shown in Fig. 1 and listed in Table 1.

Each of the 30 fish brains used in this study was screened for dopaminergic cell populations from rostral to caudal using a Zeiss Axioscope microscope with three filter set. First, the cytoarchitecture was visualized and identified with the DAPI stain, then the TH+ cell populations were visualized and photographed with the rhodamine filter set. For visualizing pS6 stained cells, the filter cube was changed to a FITC filter set and the same population photographed again. Both photographs were merged to an RGB image with the TH+ cells in the red channel and the pS6 stain in the green channel.

The images contained all TH+ cells that were found for a given area and animal. Since only every third section was stained with the double-labeling procedure and some sections were damaged, only a subset of TH+ cells could be tested for co-localization with pS6. Because some TH+ cell populations are very small, sometimes no TH+ cells could be found for a given area in an animal. However, this is not critical because the statistical test used is based on the sum of all cells per group (see below).

After all necessary images were obtained, counting was performed with the help of a custom-made program (Hofmann, MH). The user selected a brain area to be analyzed and the computer generated a random list of images to be used for counting. The counting was done blind, i.e. the user did not know from which animal group the image was selected from by the computer. The images were viewed as RGB images, but the user could also view each channel independently by pushing a key on the keyboard. This allowed for a better evaluation of double-labeling compared to the yellowish color of red and green channels combined. Frequently, the brightness of the different cells could vary in the red and green channels, and the combination would give all kinds of yellowish shades. Focusing on a cell with the red channel and switching back and forth between the red and green channels, proved to be a way more reliable to detect double-labeled cells, independently of their brightness.

First, the user marked all TH+ cells in the area of interest and then counted the number of double-labeled cells. The computer kept track of all counting and stored the value under the correct animal name, unknown to the person counting. The data were exported to a spreadsheet program and tables and bar graphs generated from there.

If the same dopaminergic cell population was detected in several different sections in the same animal, the counts were combined computationally. The entire procedure was repeated until all animals were counted. This resulted in a list with all individual TH+ cell numbers for each area and the number of double-labeled cells for each dopaminergic area and behavioral group (Isolation, Avoidance, Trained). For the micrographs shown in Fig. 3, the RGB images were split into the individual red and green channels with ImageJ to separately auto-adjust each image for brightness and contrast. The channels were subsequently combined again into a single RGB image.

2.5. Statistics and data analysis

The primary data set contained binary data, a given TH+ cell can be co-labeled with pS6 or not. Furthermore, some areas within a group were never double-labeled (0%) or always double-labeled (100%). For these kinds of data, a parametric test is not appropriate and we used the Fisher's exact test, which is designed for such cases. A matrix was created in the spreadsheet program, featuring the numbers of both double-labeled and single-labeled TH+ cells as well as the sums of the column and rows. Fisher's exact test was used to calculate whether there were significant differences in the expression pattern found among

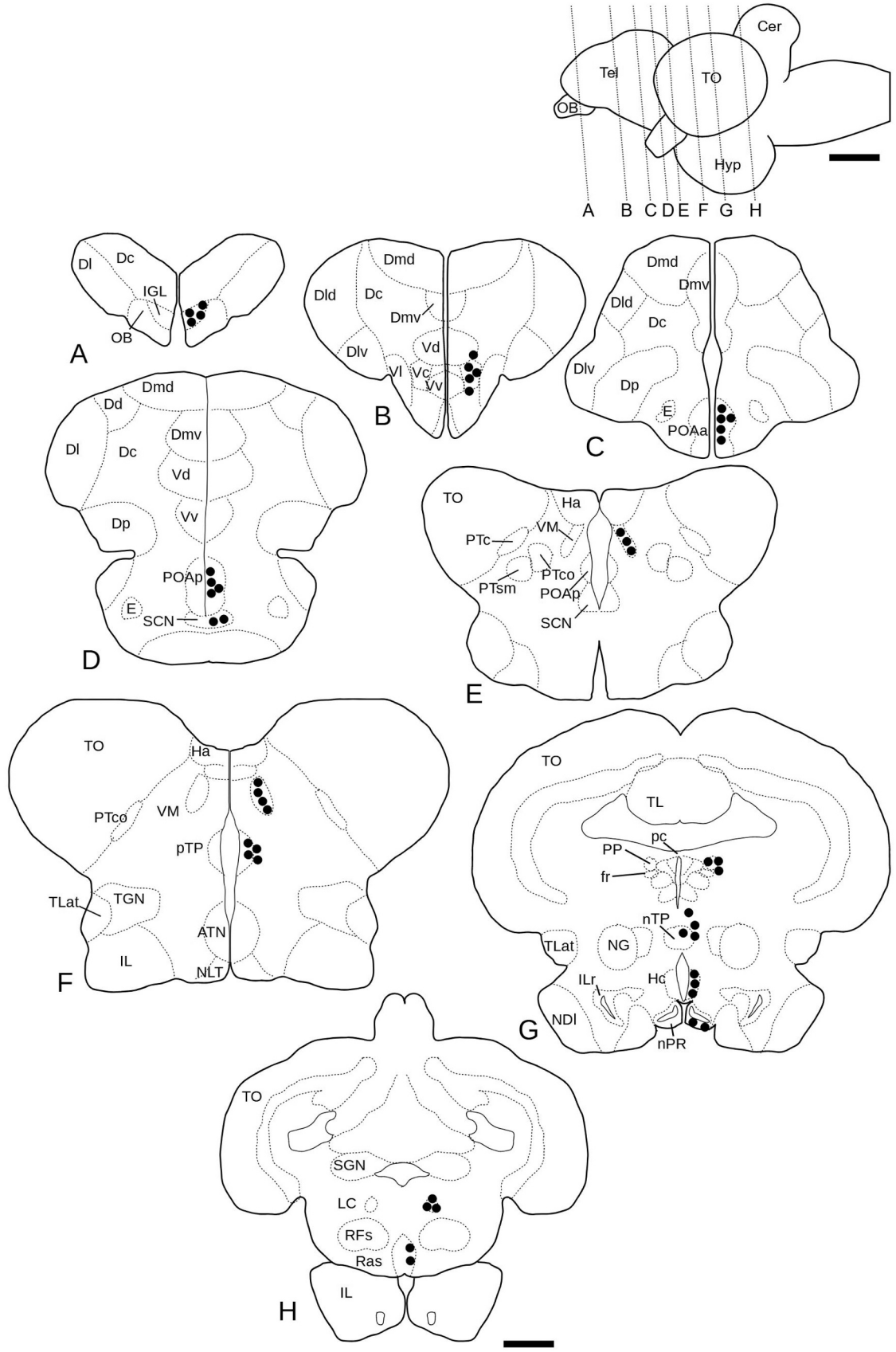

Fig. 1. Dopaminergic cell populations. Schematic drawing of the thirteen dopaminergic cell populations analyzed (see list of abbreviations). Scale bar in H equals 500 μm and applies to all cross sections. Scale bar of the sagittal view equals 1 mm. The schematic sagittal diagram of *P. zebra* brain shows the approximate locations of each section.

Tablee 1
List of brain areas analyzed.

IGL	internal granular layer of the olfactory bulb
Vc	central nucleus of the ventral division of the telencephalon
POAa	preoptic area, anterior part
POAp	preoptic area, posterior part
SCN	suprachiasmatic nucleus
VM	ventromedial thalamic nucleus
pTP	periventricular posterior tuberculum
PP	periventricular pretectal nucleus
nTP	nucleus of the posterior tubercle
Hc	caudal hypothalamus
nPR	nucleus of the posterior recess
LC	locus coeruleus
Ras	raphe superior

Avoidance, Trained, and Isolation groups. A significant level of $p < 0.05$ was chosen to reject the null hypothesis. Details on the Fisher test can be found in the supplementary materials. In addition, the non-parametric Mann-Whitney-test was calculated to test for group differences.

We used the R package pheatmap (Kolde, 2012) to perform hierarchical clustering analyses of the dataset, clustering both individuals and double-labeled TH+ cell populations, using average linkage as agglomeration method and correlation as distance metric. Using the R package pvclust (Suzuki and Shimodaira, 2006), we then estimated the robustness of any resulting clusters by multiscale bootstrap resampling. Clusters for which $p < 0.05$ are indicated with bootstrap values ≥ 95. Because of the multivariate nature of the dataset, we conducted a Principal Components Analysis (PCA) in R. For the PCA and cluster analysis, it was necessary to replace missing values. We calculated the mean and standard deviation within each brain area and group and replaced missing values with a Gaussian random number created from the mean and standard deviation. This would preserve the mean and also the variance in the data set. Since there is a high number of missing values in some areas, we tested the procedure by creating 1000 data sets of random numbers and checked for variability in the first principle component of the PCA. There were little variations in the loadings of the components and the PCA was very robust and reproducible (see Fig. S2).

3. Results

3.1. TH immunoreactive cell populations

The distribution of dopaminergic cell bodies in the brain of *P. zebra* was investigated with an antibody against TH and DAB as a chromogen. All major cell populations identified (Figs. 1, 2) were then used to study dopamine activation in three behavioral contexts, i.e. isolation, avoidance and visual discrimination learning. Differences in cell morphology and cell size were not measured systematically, but Fig. 2 shows high magnification photographs of all areas.

The first population of TH immunoreactivity was found in the olfactory bulb, internal granular layer (IGL, Figs. 1A, 2A). While TH+ cell bodies were found in the cellular (granular) layer, fibers were localized in the mitral layer. A population of large TH+ cell bodies extended along the medial olfactory tract and many more were located in the central nucleus of the ventral division of the telencephalon (Vc, Figs. 1B, 2B).

Two prominent TH+ cell populations were located in the preoptic area. An anterior population between the anterior commissure and the beginning of the optic chiasm (POAa, Figs. 1C, 2C) was distinguished from a more posterior population (POAp, Figs. 1D, 2D). At the level of the rostral POAp population, the suprachiasmatic nucleus contained also some TH+ cells (SCN, Figs. 1D, 2E).

A large number of small TH+ cell bodies was located in the ventromedial thalamic nucleus (VM, Figs. 1E-F, 2F). Their fibers seemed to be orientated dorsolateral, towards the tectum opticum. More caudally, another cell population was present in the periventricular pretectal nucleus just below the posterior commissure, dorsal to the fasciculus retroflexus (PP, Figs. 1G, 2H). It extended caudally along the posterior commissure. More caudally, TH+ cell populations were observed above the tract of the posterior commissure, but those cells seemed to be continuous with the ventral cell population and are thus also part of PP. Additional TH immunoreactivity was found in the cells of the periventricular posterior tuberculum (pTP, Figs. 1F, 2G). This population showed large cells with fibers oriented lateral and seemed to extend into a small tract visible between the lateral end of the tectum opticum and the torus lateralis. This tract could be followed into the brain stem (data not shown).

Scattered big TH+ cells were found more caudally and ventrally to the pTP. They showed fibers larger than the ones of the pTP, with extensions into the brain stem tract (Figs. 1G, 2I). However, many of the fibers followed a more dorsal route. Although these cells are located in the area of the nucleus of the posterior tubercle (nTP), they constitute only a subset of cells of the nTP.

Ventral to the nTP, two further populations of TH+ cells were found. Small cells were found along the ventricle in the periventricular caudal hypothalamus (Hc, Figs. 1G, 2J). A small number of weakly stained cells were also present around the posterior recess (nPR, Figs. 1G, 2K).

At the isthmic region, a small number of very large cells were TH+ and identified as the locus coeruleus (LC, Figs. 1H, 2L). TH is present in all cells that produce catecholamines. Dopamine is produced in all forebrain areas; the locus coeruleus is the only cell population that produces noradrenaline. Although our study focuses on the dopaminergic system, we included the locus coeruleus because it is also an important modulatory system and was stained with both TH and pS6 antibodies.

At the same level, smaller TH+ cells were located along the midline, identified as the raphe superior (Ras, Figs. 1H, 2M).

Other TH+ cell populations were present in the vagal region in the brain stem, but were not included in this study. There were also some TH+ cells in the paraventricular organ, but they were very weakly stained and visible in only a few individuals. Therefore, this region was not included in our study.

3.2. Co-localization of TH and pS6

Examples of cell populations analyzed for co-localization of pS6 and TH-+ are shown in Fig. 3. Co-localization of the two proteins was visualized by the overlap of the two secondary antibodies' colors (green for pS6 and red for TH), resulting in a yellowish colored cell. The experimental groups are shown in different columns, i.e. Isolation, Avoidance, Trained, from left to right.

3.2.1. Isolation group

In the cell populations of the Isolation group (Fig. 3 "Isolation" column, A1-M1), there was little co-localization of TH and pS6. A few cells showed co-localization in the nPR (Fig. 3, K1) and all cells in the locus coeruleus were double-labeled (Fig. 3, L1).

3.2.2. Avoidance group

The Avoidance group (Fig. 3 "avoidance" column, A2-M2) showed the biggest number of cell populations with double-labeled cells compared to the Isolation and the Trained group. In particular, co-localization of TH and pS6 was found in Vc (Fig. 3, B2), POAa (Fig. 3, C2), POAp (Fig. 3, D2), SCN (Fig. 3, E2), VM (Fig. 3, F2), pTP (Fig. 3, G2), PP (Fig. 3, H2), nTP (Fig. 3, I2), Hc (Fig. 3, J2), LC (Fig. 3, L2) and Ras (Fig. 3, M2).

3.2.3. Trained group

In the Trained group (Fig. 3 "trained" column, A3-M3) co-localization of TH and pS6 was found in cells of pTP (Fig. 3, G3), PP (Fig. 3, H3), nTP (Fig. 3, I3), LC (Fig. 3, L3) and Ras (Fig. 3, M3).

Besides direct co-localization of TH and pS6, there was a marked increase of pS6-ir cell bodies in some areas, especially in the Avoidance

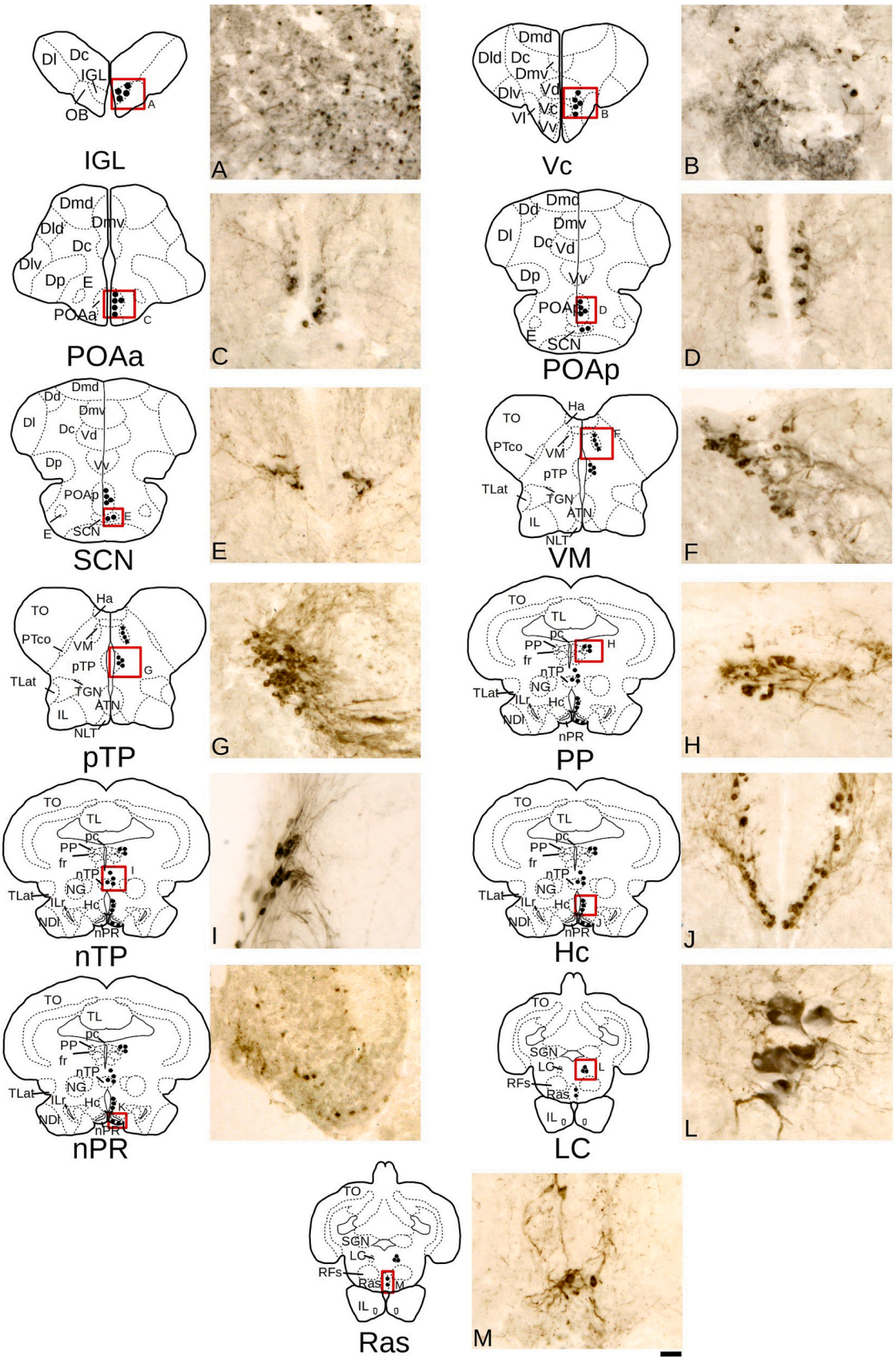

Fig. 2. Representative micrographs (A-M) of the dopaminergic cell populations investigated. On the left of each micrograph, a drawing highlighting the localization in the brain of the respective cell population is shown. Scale bar: 50 μm.

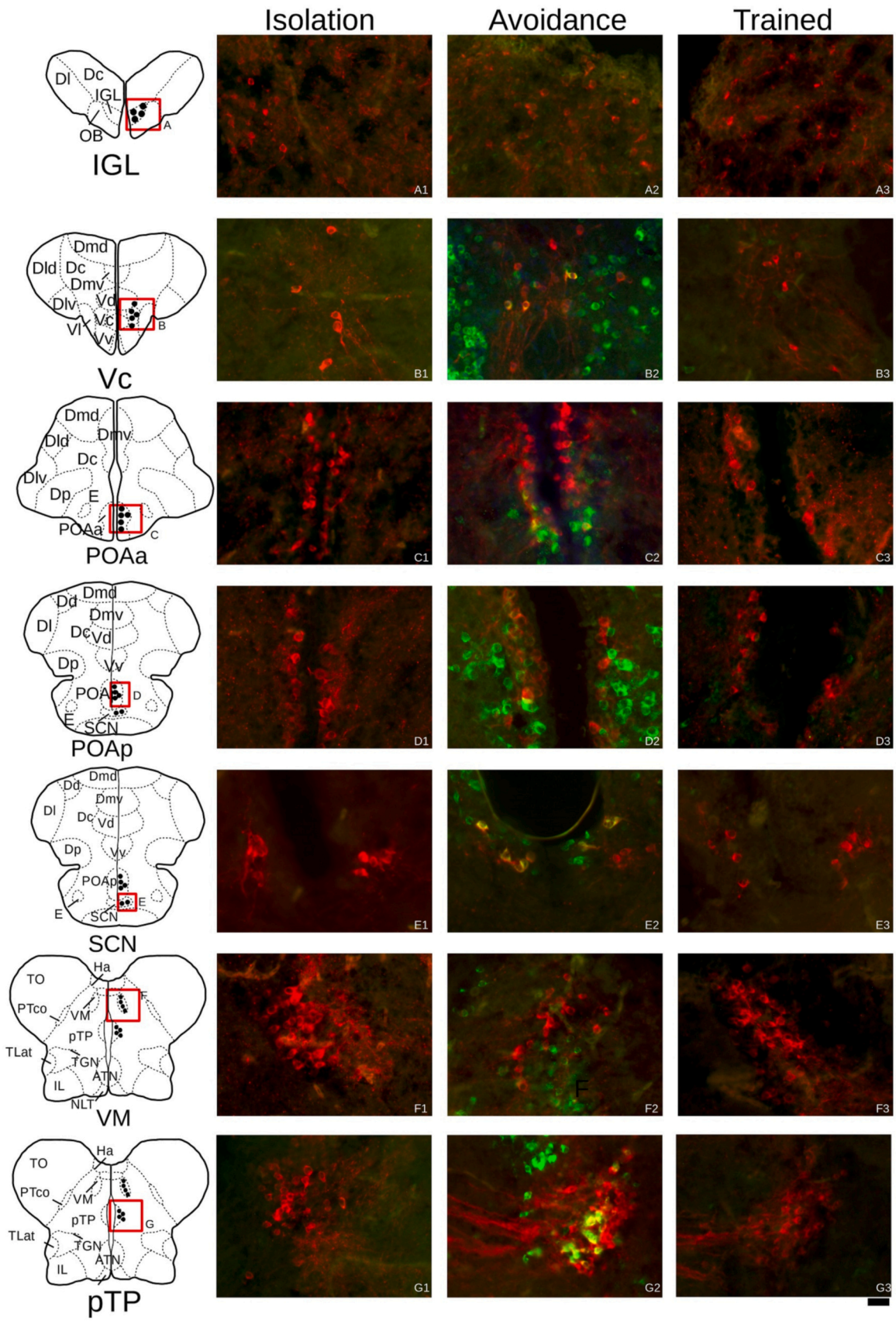

Fig. 3. Double-labeling micrographs. Double-labeling (yellow) of pS6 (green) – TH (red) in the three different groups (Isolation, Avoidance and Trained) in the thirteen dopaminergic cell populations analyzed (IGL, Vc, POAa, POAp, SCN, VM, PP, pTP, nTP, Hc, nPR, LC, Ras – see list of abbreviations). Scale bar: 20 μm.

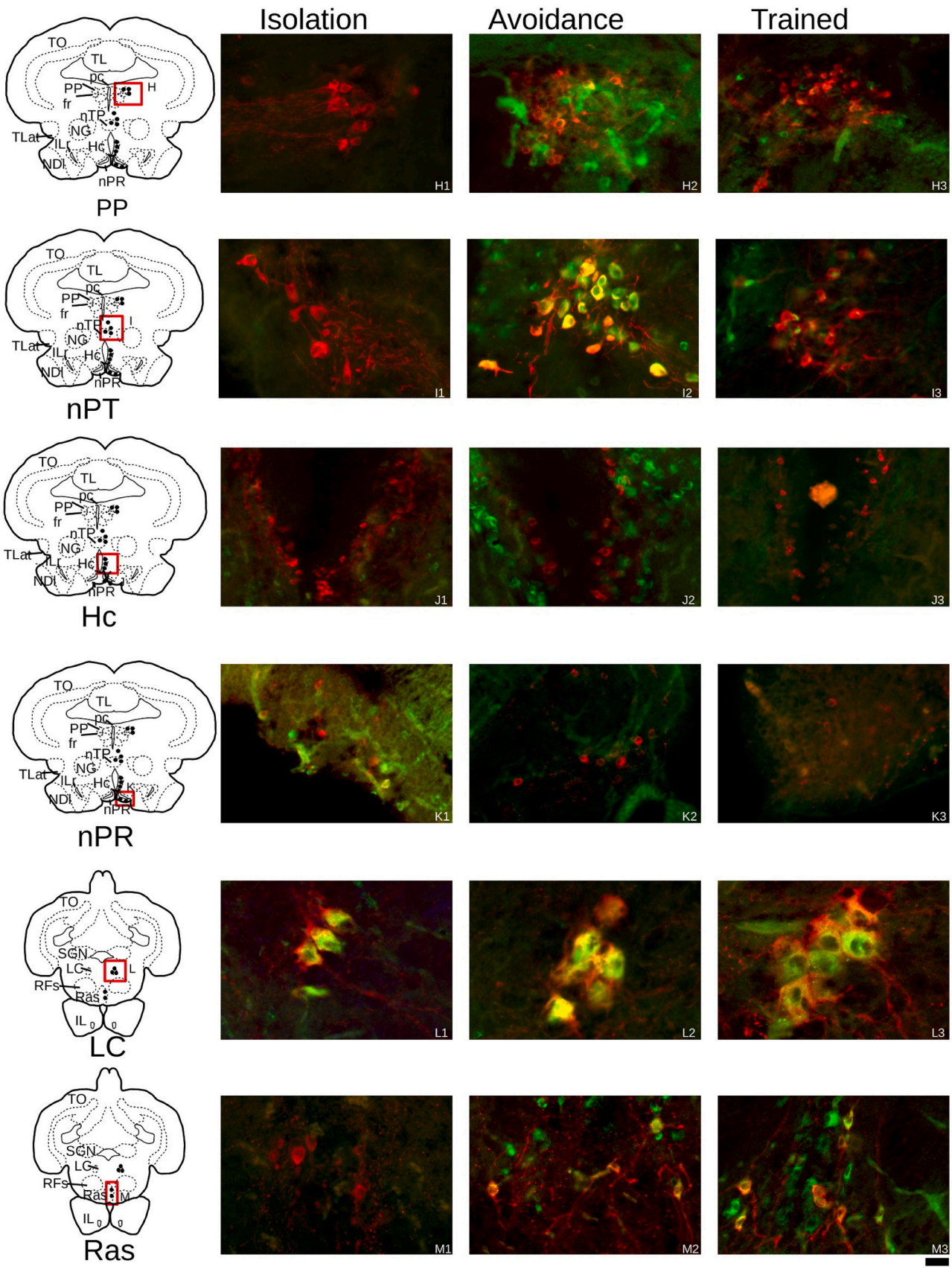

Fig. 3. (*continued*).

group. Sometimes, the additionally labeled pS6 cell bodies were located in between the TH+ cells, often they were found around the TH+ cell population. This could be seen in the POAa (Fig. 3, C) and POAp (Fig. 3, D), the PP (Fig. 3, H), and the Hc (Fig. 3, J) populations. Here, there was an increase in double-labeled cells, but there were many more additionally activated pS6 labeled cells that were not TH+ . In the nTP, almost all cells were double-labeled in the Avoidance group and no cells were exclusively pS6 labeled. In the SCN, half of the TH+ cells were stained for pS6, with many additional cells that only showed pS6 stain.

3.3. Quantification of co-localization

For quantification, the number of TH+ cells in the different areas and the number of TH+ cells that were double-labeled with pS6 antibodies were counted. Fig. 4A shows the percentage of double-labeled cells for each animal and Fig. 4B the averages in each area for the three experimental groups. In Fig. 4C, the differences are visualized in a bubble chart and Fig. 4D lists the p-values calculated according to the Fisher and Mann-Whitney tests. Detailed information about the raw data, the actual cell counts, and statistical tests can be found in the supplementary material. The Avoidance group showed the majority of the double-labeled cell populations. The large cells in the nTP showed the largest extent of activation. A strong activation was found also in the SCN, compared to the Isolation group. The Avoidance group showed an increase in double-labeled cells also in almost all other TH+ areas, except the IGL, where no activation was detected. The nPR cell population was the only area where fewer double-labeled cells were found relative to the Isolation group. In the locus coeruleus almost all big cells were double-labeled, in all groups. This is in contrast to the Ras, which showed a strong activation in both the Avoidance and the Trained group, but not in the Isolation group.

In addition to the Ras, the Trained group showed an increase of activation in the PP and the nTP. In the PP, the activation was not strong, similar to the Avoidance group. In the nTP, there was less activation than in the Avoidance group, but still significantly more than in the Isolation group.

3.4. Co-activation patterns of dopaminergic cell populations

Above, we described the average group values of the activation of TH+ cells in the different brain areas, but the variations within each group was not taken into account. Fig. 4A shows the individual values within each group and area, which shows that the response is sometimes very heterogeneous and nonlinear. This is especially apparent in the SCN in the Avoidance group and the nTP in the Trained group. Some animals showed zero activation whereas others showed a high proportion of double-labeled cells. The Fisher test does not take this into account, but other statistical tests are not compatible because the data are not normal distributed, variances are not equal between groups, and there are many zero values in the data set. The non-parametric Mann-Whitney test shows some agreement with the Fisher test, but it is not applicable in some cases with many zero values (ties in the ranks). However, there are two other methods that we used to investigate the variability of the animals. These are based on the pattern of activation in all brain areas rather than on investigating each area separately.

First, we conducted a Principal Components Analysis (PCA) to identify the double-labeled TH+ cell populations that most strongly separated the experimental groups. We discovered that principal component (PC) 1, which explained 69.0% of the variance (Fig. 5A), significantly clustered the three experimental groups from each other (ANOVA: F27, 2 = 135.4, p = 8.4 * 10–15; Fig. 5D, E). This clustering was largely driven by the nTP cell population as well as, to a lesser extent, by double-labeled TH+ in the SCN and raphe (Fig. 5B). The three groups can be separated by the first component alone with no overlap (Fig. 5E). Double-labeled TH+ in the SCN and raphe loaded even more strongly on PC2 (Fig. 5C), which further separated the Trained group from both the Isolation and Avoidance groups (ANOVA: F27, 2 = 17.95 p = 1.1 * 10–5; Fig. 5F).

The second analysis was a hierarchical clustering that is grouping the animals by similarity in their activation pattern. The cluster analysis itself is not aware of any group memberships, but a post-hoc visualization showed that the cluster analysis reconstructed the groups almost perfectly with just two animals misplaced into the wrong group (Fig. 6).

4. Discussion

4.1. Dopaminergic cells distribution and double-labeling

The dopaminergic system is well investigated in many vertebrate groups mainly by using antibodies against tyrosine hydroxylase (TH), the enzyme that catalyzes the rate limiting step in catecholamine synthesis (Fernstrom and Fernstrom, 2007) and thus present in all cells producing catecholamines. In the brain, noradrenaline is found only in the locus coeruleus and all TH+ cell populations rostral to the brain stem are considered to be dopaminergic (Ma, 1994). There are several TH+ cell populations described, extending from the olfactory bulb and preoptic area into the di- and mesencephalon, as well as rhombencephalon and spinal cord. In mammals, an A1-A17 classification scheme has been established (Lindvall and Björklund, 1984; Hökfelt, 1984; Smeets and González, 2000; Nagatsu, 2007). Studies in fish have mainly used a teleost-specific nomenclature (see references below), even though more recent studies in zebrafish have adopted the mammalian classification. To facilitate the comparison with older fish literature, we use here the traditional terminology. The areas we identified in *P. zebra* correspond well to other studies in a variety of fish species (*Carassius*, Hornby et al., 1987; *Anguilla*, Roberts et al., 1989; *Apteronotus*, Sas et al., 1990; *Clarius*, Corio et al., 1991; *Dicentrarchus*, Batten et al., 1993; *Salmo*, Manso et al., 1993; *Gnathonemus*, Meek et al., 1993; *Solea*, Rodríguez-Gómez et al., 2000; *Danio*, Rink and Wullimann, 2001; *Rhodeus*, Pushchina, 2009; *Poecilia*, Parafati et al., 2009; Filippi et al., 2010; *Astatotilapia*, O'Connell et al., 2011; O'Connell et al., 2013a; *Cirrhinus*, Kumar et al., 2014; *Porhichtys*, Goebrecht et al., 2014; *Nothobranchus*, Borgonovo et al., 2021).

Although the location of the cell populations and the distribution of their processes is well known, specific connections of TH+ cells are not known and additional studies are required. Moreover, little is known about the function of the different subsystems in teleost fish. Activation markers have been used to study some subcomponents, but the more commonly used nuclear markers c-fos and egr-1 may not be expressed in all dopaminergic systems. In contrast, the ribosomal marker pS6 shows activation in many more areas (Calvo et al., 2023). We investigated here the activation of TH+ cells in 13 different areas in two experimental groups and the Isolation group. This shows for the first time how different behavioral situations are changing the balance between the different dopaminergic subsystems that all act together to determine the complex emotional, motivational, and hormonal state of the animal.

The activation of TH+ cells shows considerable variations both between but also within groups. In some areas, some animals within a group may show no activation whereas others had a high percentage of double-labeled cells. This may be due to nonlinear response properties. In addition, many areas showed zero activation, particularly the Isolation group. This made it difficult to find an appropriate statistical test. Tests based on normal and equal distributions are not appropriate whereas non-parametric tests based on ranks do not take the magnitude of the activation into account and values with many zeros (ties) are problematic. The Fisher exact test was used to test for significant differences here. In this test, all TH+ cells found in all animals of a group were pooled for each brain area and the number of double-labeled cells compared among groups. The Fisher test can be applied for such data, but it ignores all within-group variations. The non-parametric Mann-Whitney test can compare within-group variations based on ranks, but fails in cases with many zero values (ties in the ranks). As an alternative

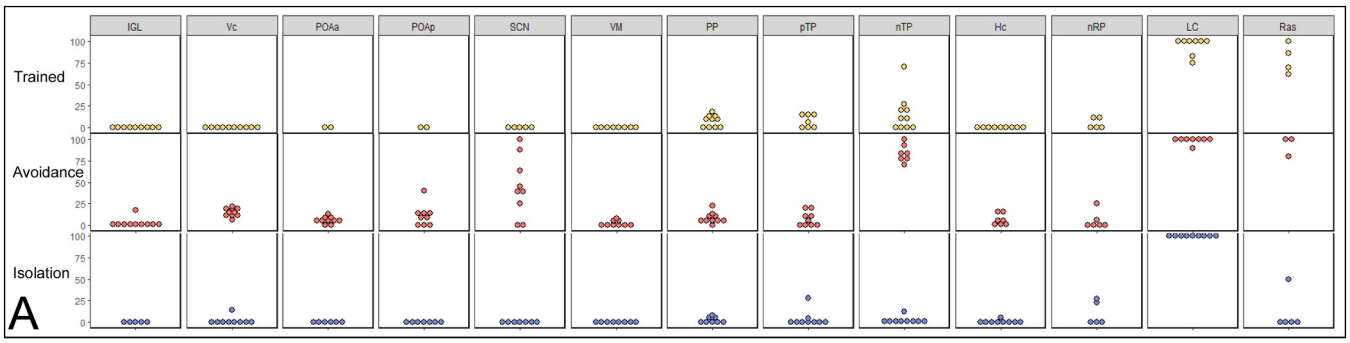

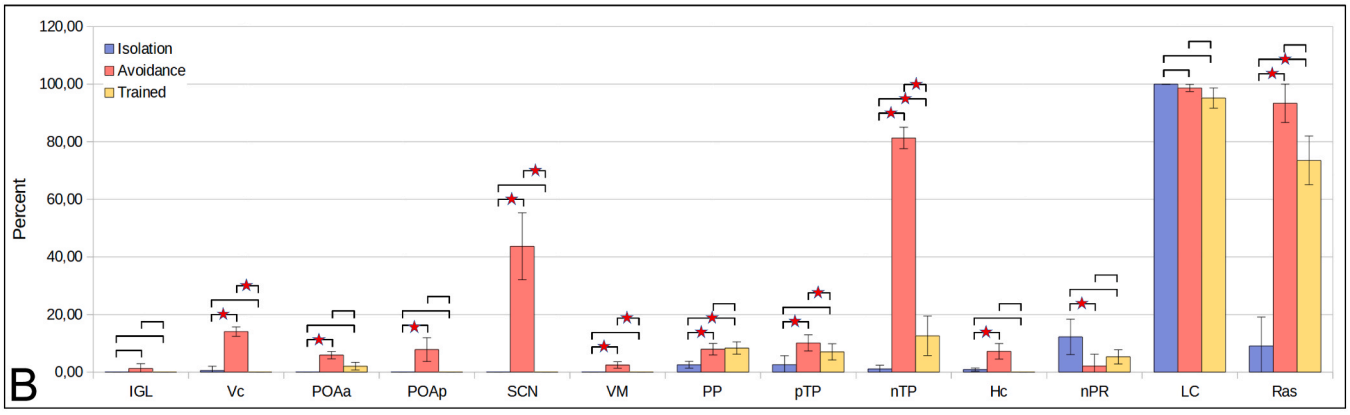

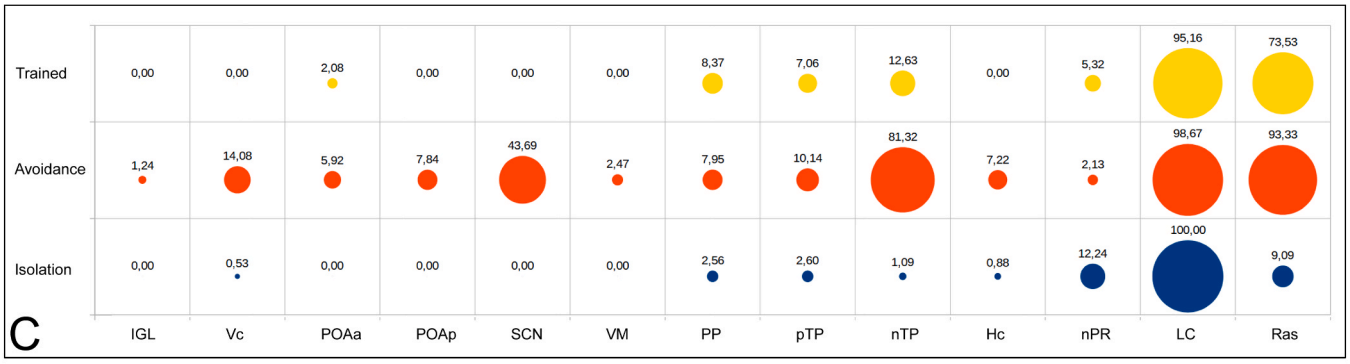

Fisher Test

A / I	IGL	Vc	POAa	POAp	SCN	VM	PP	pTP	nTP	Hc	nRP	LC	Ras
p	0.06856336	0.00000001	0.00294038	0.00082442	0.00000000	0.01006037	0.00000635	0.00001009	0.00000000	0.00026908	0.02194826	0.57692308	0.00020475
p (adj)	0.89132368	0.00000010	0.03822488	0.01071742	0.00000000	0.13078476	0.00008256	0.00013112	0.00000000	0.00349798	0.28532736	7.50000000	0.00266169
T / I													
p	1.00000000	0.45563549	0.30000000	1.00000000	1.00000000	1.00000000	0.00083635	0.61285344	0.00000428	0.21573120	0.19406209	0.14538884	0.00000170
p (adj)	13.00000000	5.92326139	3.90000000	13.00000000	13.00000000	13.00000000	0.01087252	7.96709476	0.00005569	2.80450554	2.52280719	1.89005497	0.00002204
A / T													
p	0.15286155	0.00003466	1.23760986	1.04090211	0.00022006	0.04396242	1.64958881	0.00411084	0.00000000	0.99829634	0.28100000	0.56894654	0.11169625
p (adj)	1.98720014	0.00045061	16.08892822	13.53172739	0.00286073	0.57151143	21.44465458	0.05344086	0.00000000	12.97785238	3.65300000	7.39630497	1.45205129

Mann-Whitney

A / I													
p	0.2189117	0.000145369	0.00355367	0.00910504	0.00265082	0.09184881	0.01558781	0.19472538	0.00017482	0.01696521	0.7512481	0.29084962	NA
p (adj)	2.8458521	0.001889797	0.04619771	0.11836552	0.03446066	1.19403453	0.20264153	2.53142994	0.00227266	0.22054773	9.7662253	3.78104506	NA
T / I													
p	NA	0.31885944	NA	NA	NA	NA	0.11840682	0.20507806	0.20507806	0.34798425	0.60096879	0.11517662	NA
p (adj)	NA	4.14517272	NA	NA	NA	NA	1.53928866	2.66601478	2.66601478	4.52379525	7.81259427	1.49729606	NA
A / T													
p	0.9049317	0.0001	NA	NA	0.01083507	0.09184881	0.97011415	0.99822141	0.00017538	0.00222908	1.06277096	0.483576775	NA
p (adj)	11.7641121	0.0013	NA	NA	0.14085591	1.19403453	12.61148395	12.97687833	0.00227994	0.02897804	13.81602248	6.286498075	NA

D

Fig. 4. Charts of the activation of the 13 dopaminergic cell populations. A: Dot plot showing the activation of all animals of the three groups for each brain area in percent on the y axis. Individual animals are spread out in the x axis if they have the same value. B: Mean percent of co-localization of pS6 and TH in all three groups. A star indicates significant ($p < 0.05$) differences according to the Fisher test between the groups. C: Bubble plot of the activation data showing the percent of activated TH+ cells in the three groups as a matrix with the size of the circles reflecting the magnitude. D: p-values according to the Fisher test and the Mann-Whitney test for all brain areas and all possible group combinations. P (adj.) are the Bonferroni adjusted values. Green cells indicate p-values < 0.05. All original values and cell counts can be found in the supplementary materials. The Fischer test has always one degree of freedom.

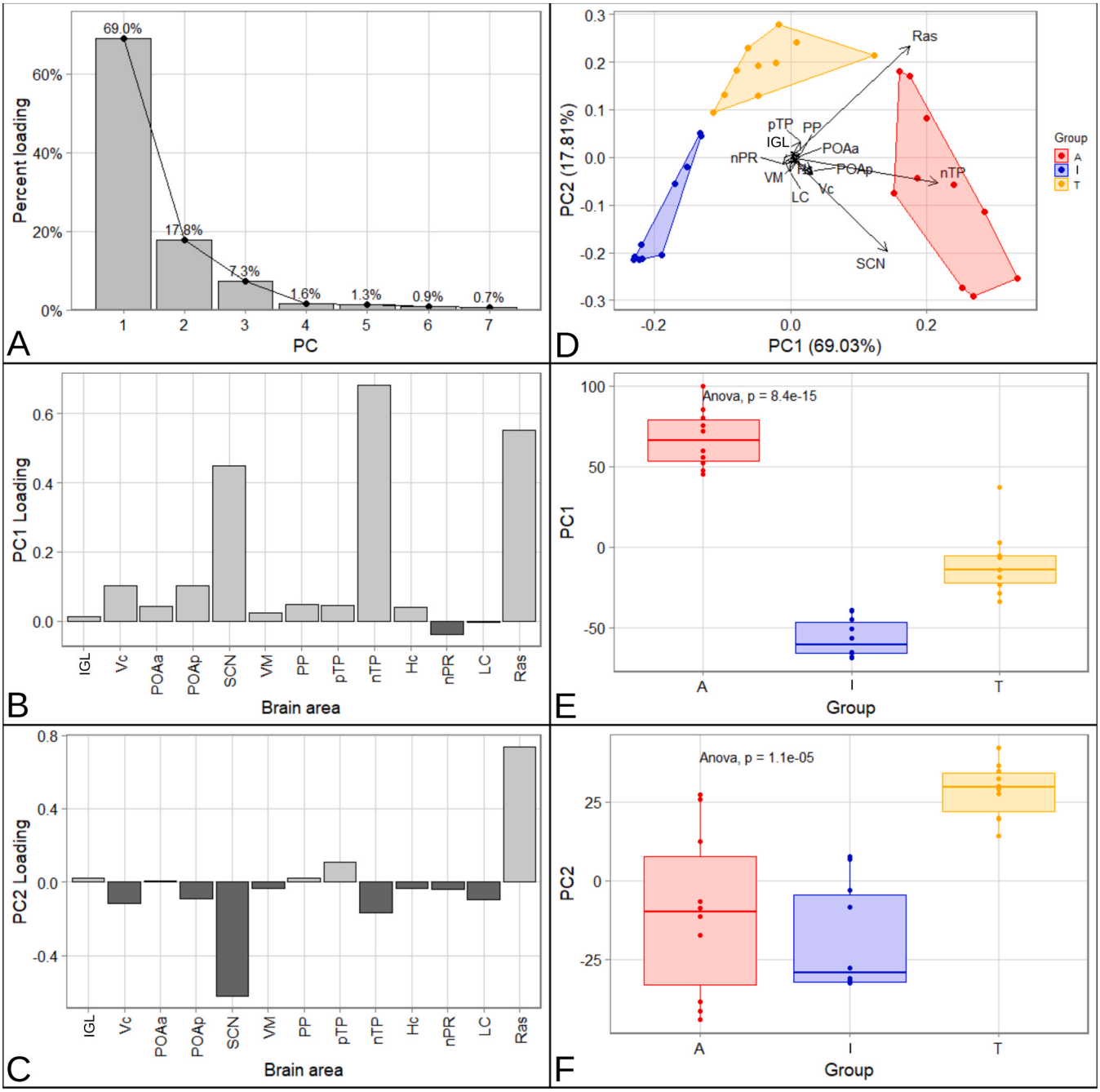

Fig. 5. PCA analysis of the activation in the 13 dopaminergic cell populations. (A) shows that the first component contains most of the variances in the data set. (B) shows the different contributions of the areas to the first component (PC1) and (C) the composition of the second component (PC2). The scatter plot in (D) shows the location of the groups with the PC1 and PC2 space. The differences between groups are mostly caused by SCN, nTP, and Ras in PC1. PC2 can still separate the Trained group from the others. (E) shows the box plots of the groups on the PC1 axis and (F) on the PC2 axis. All three groups can be separated by PC1. The Trained group is different from the others in PC2 due to the activation of Ras and a lack of activation in SCN in contrast to the strong activation in the Avoidance group. Groups are abbreviated as Isolation 'I', Avoidance 'A' and Trained 'T'. See Table 1 for a list of brain part abbreviations. Axes in D are scaled eigenvalues.

to statistical tests, we made a principle component analysis and a cluster analysis that are both based on the pattern of activation in all brain areas.

The data for each of the 30 animals were analyzed with these methods that are initially not aware of any group memberships. The PCA showed in the first two components the combination of areas with the largest variance in the data set. When these data are plotted in a scatter plot and post-hoc color coded for groups, it becomes clear that the largest variations in the data set are due to group differences. This was tested with an ANOVA. An ANOVA is possible now because the values for the ANOVA are the sum of the weighted reconstructions of the principle components. This clearly showed that the different treatments (groups) are dominating the variances seen in the data set and not the within-group variances. In fact, the first principle component is very similar to the actual group differences shown in Fig. 4B.

The second analysis we performed was the cluster analysis. Here, all 30 animals were analyzed and grouped by the similarities based on their activation pattern. A post-hoc color coding shows that the activation pattern is highly characteristic for each group. Only two animals were assigned to the wrong clusters.

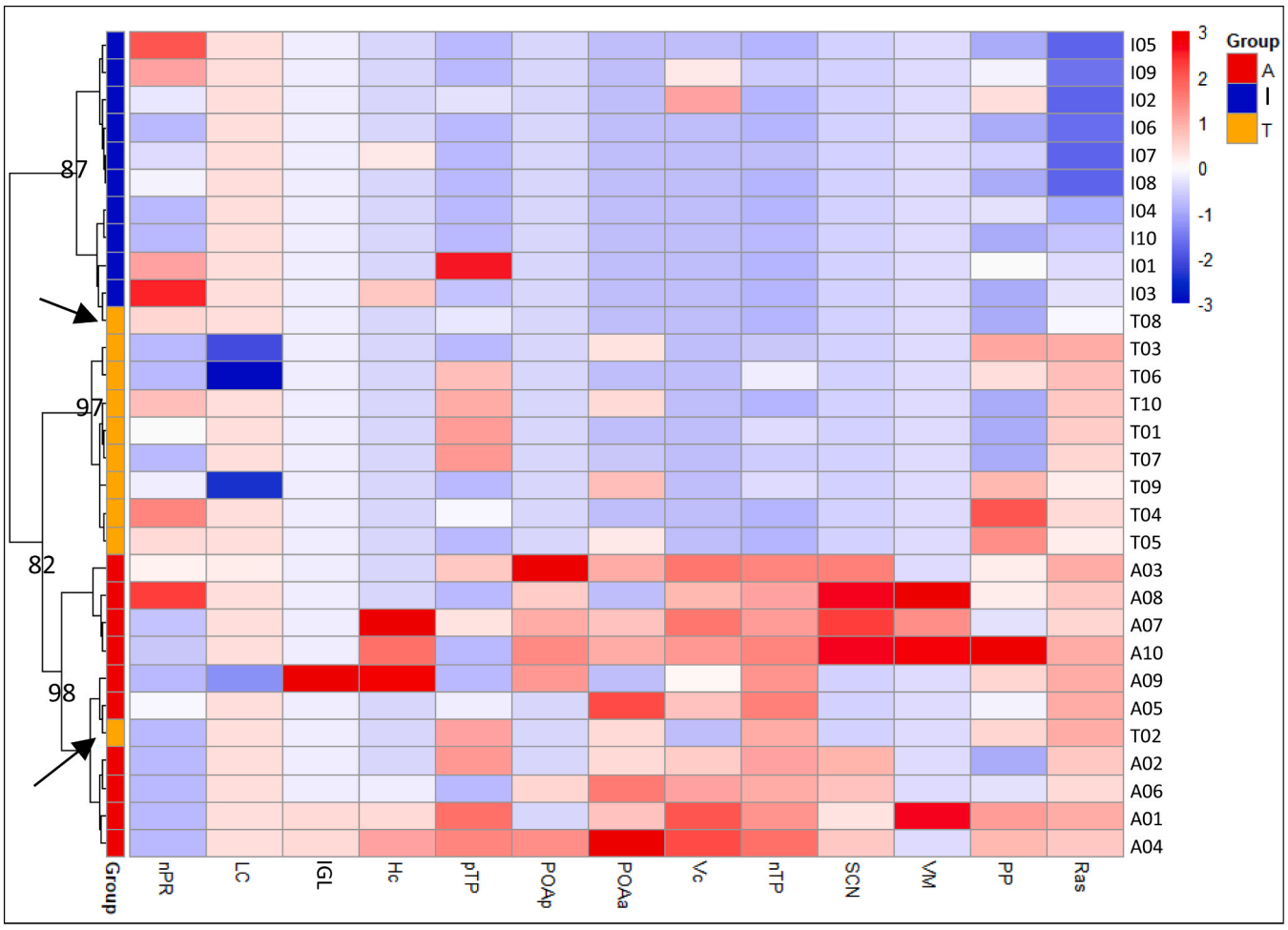

Fig. 6. Hierarchical cluster analysis of the data set. The animals are grouped according to the similarity of the activation pattern of TH+ cell populations. The heatmap of the activity pattern of each animal is scaled by column. Numbers on the dendrogram represent the p-values of the branchings. The color code next to the dendrogram shows the group assignments of the animals. The cluster analysis was reconstructing the correct groups almost perfectly, there were only two animals belonging to the Trained group that were clustered incorrectly (arrows).

Both, the PCA and the cluster analysis showed that there is a distinct pattern of the percentages of double-labeled TH+ cells that is group (treatment) specific. Although the activation of a single area in a given animal can be highly variable, the combined pattern across all areas is highly characteristic for each group.

4.1.1. *Telencephalic cell populations*

A large population of TH+ cells was located in the olfactory bulb as in all other vertebrates investigated so far. Other TH+ cells are located in different ventral telencephalic areas. In our material, most cells were found in the Vc and those were used to quantify double-labeling with pS6. Ventral telencephalic TH+ populations were found in all other studies in fishes, but their assignment to the different ventral areas differs. Some authors located also TH+ cells in Dc (Hornby et al., 1987; Roberts et al., 1989; Piñuela and Northcutt, 2007; O'Connell et al., 2011; O'Connell et al., 2013a), in Dp (Piñuela and Northcutt, 2007; O'Connell et al., 2011), in Dl (O'Connell et al., 2011; O'Connell et al., 2013a), and in Dm (Piñuela and Northcutt, 2007). TH+ cell populations in the telencephalon in addition to the IGL were also found in elasmobranchs (Meredith and Smeets, 1987), lampreys (Pierre et al., 1997; Pombal et al., 1997), and lungfish (Reiner and Northcutt, 1987) and seem to be basal vertebrate characteristic that was lost in tetrapods.

In our study, a specific activation of the TH+ cells was not found in the olfactory bulb although general pS6 activity did increase in the IGL in the Avoidance group (Calvo et al., 2023). Apparently, the pS6 activation did not affect the TH+ cells in the IGL. In contrast, the ventral telencephalic cell population (Vc) showed a specific activation of the TH+ cell population in the Avoidance group. The functional significance of this activation is not clear. The medial olfactory tract sends fibers into the area and the ventral telencephalon responds well to olfactory stimulation. However, there are projections from many other areas to the ventral telencephalon that could also affect the TH+ cells in this region. Most processes of the ventral telencephalic TH+ cells course laterally to innervate heavily Dp (O'Connell et al., 2011). This would indicate a modulation of information processing in the Dp. Interestingly, unilateral olfactory deprivation in zebrafish led to a down regulation of TH+ cells in the olfactory bulb but did not show changes in the ventral telencephalon (Kress and Wullimann, 2012) as indicated with co-localization of TH+ cells with egr-1. However, this study is not directly comparable to ours, as Kress and Wullimann (2012) investigated larval zebrafish that are about to be imprinted to kin odors and they used the nuclear marker egr-1, which is acting at a different level compared to the ribosomal pS6 marker.

4.1.2. *Preoptic-hypothalamic system*

TH+ cells in the preoptic-hypothalamic area are located in four specific populations, the POAa, POAp, Hc, and nPR. These areas are known to be involved in hormonal control and stress response acting on the pituitary (Tuomisto and Männistö, 1985; Semenova et al., 2014; Fontaine et al., 2015). The dopaminergic neurons of the POAa are

known to regulate the production of gonadotropin releasing hormone (GnRH) in an inhibitory way. In stressful situations, an increased dopaminergic level suppresses the production of GnRH, which in turn downregulates the release of gonadotropins in the pituitary (Kah et al., 1984; Kah et al., 1986; Kah et al., 1987; Anglade et al., 1993; Linard et al., 1996; Weltzien et al., 2006; Chabbi and Ganesh, 2015; Bhat and Ganesh, 2020). Dopaminergic cells in the nucleus of the posterior recess project directly to the pituitary and control the release of prolactin. Higher dopamine release suppresses the production of prolactin from the pituitary (Ben-Jonathan, 1985; Anthony et al., 1993; Freeman et al., 2000; Torner, 2016). It has been demonstrated that restraint stress in rats causes a decrease in the tubero-infundibular activity of dopaminergic neurons, with a consequent increase of circulating levels of prolactin (Shin, 1979; Moore et al., 1987). Thus, in stressful situations the dopaminergic activity in the POA would rise to suppress the release of gonadotropins and the dopamine production in the tubero-infundibular system would decrease to allow higher prolactin levels. This is exactly what we found in the Avoidance group. The POA TH+ cells showed higher pS6 co-localization but in the nPR co-localization was lower than in the Isolation group, indicating a deactivation. In the Trained group, no differences were found in both the POA cell populations or nPR.

4.1.3. Suprachiasmatic nucleus

Although we know the suprachiasmatic nucleus should be included in the "preoptic-hypothalamic system", we found it necessary to discuss it as a separate system, as the SCN contains the main pace maker of the circadian clock, which synchronizes other clock oscillators in the brain and throughout the body (Reppert and Weaver, 2002; Lowrey and Takahashi, 2011; Lu and Kim, 2022). The most important signal for the entrainment of circadian rhythms is light. The responses of several brain areas to photic stimulation have been well studied in many animals (e.g. Enger, 1957; Takeuchi et al., 1991; Leard et al., 1994). The effect of non-photic stimulations is mainly studied in mammals (Tahara and Shibata, 2018). Especially arousal stimuli like handling, social interactions, locomotor activity, and stress can change the circadian rhythm in mice and hamster (Antle, Mistlberger, 2000; Mistlberger and Skene, 2004; Mistlberger and Antle, 2011). Some studies in goldfish showed that different feeding times can be remembered (Sánchez-Vázquez et al., 1997; Sunuma et al., 2009). This shows that events can be associated relative to the circadian clock.

In some vertebrates, an important signal to synchronize different clock oscillators in the brain is dopamine (Mendoza and Challet, 2014; Moore and Whitmore, 2014; Korshunov et al., 2017; Grippo et al., 2020). In the present study, there was strong activation of TH+ cells in the SCN in the Avoidance group. Although there was no change in the light regime in our experiments, the timing of a strong event relative to the circadian clock may be an important signal that leads to an activation of the SCN.

4.1.4. Ventral thalamic and pretectal populations

In the diencephalon there are two dorsal cell populations with a large number of TH+ cells. One was located in the ventral thalamus (VM) and the other one in the periventricular pretectum adjacent to the posterior commissure (PP). Dopaminergic cells in the ventral thalamus were found in most other studies in fish. They may correspond to the VM of Ito et al. (1986), who investigated the connections of this nucleus in Rockfish *Sebastiscus marmoratus*. The VM receives inputs from many sources including the retina, TS, TO and telencephalon and it projects back to many of them. The specific connections of the TH+ cells are not known.

TH+ cells in the PP were also reported in many other fishes. Less is known about the connections of this cell population, but tracer injections into the tectum opticum consistently labeled cells in this area (Grover and Sharma, 1981; Luiten, 1981; Fiebig et al., 1983; Striedter, 1990; Schlussman et al., 1990; Perez-Perez et al., 2003; de Arriba and Pombal, 2007). Although double-labeling with TH antibodies was not done in those tracer studies, it seems the VM and PP are the major source of TH+ fibers in the tectum opticum and probably also to the torus semicircularis. The tectum opticum (colliculus superior) receives also dopaminergic projections in mammals. One source of these fibers is TH+ cells in the zona incerta (Bolton et al., 2015), which may not be homologue to the VM or PP in fishes. In reptiles and birds, cell populations were present in a location that could correspond to the PP of fishes (Smeets et al., 1986; López-García et al., 1992; Rodman and Karten, 1995). Although the homologies of the dopaminergic cells projecting to the tectum opticum is uncertain across vertebrate groups, studies in mammals show that information processing in the tectum (colliculus superior) is modulated by dopamine (Takakuwa et al., 2017; Valdés-Baizabal et al., 2020; Montardy et al., 2021). Our study showed an activation of PP in the Avoidance and Trained groups and an additional, although low, activation of VM in the Avoidance group only. This may indicate a specific modulation of tectal and/or toral information processing possibly due to the visual stimulation present in both groups.

4.1.5. Posterior tubercle

There were two TH+ cell populations in the posterior tubercle in our fish. One was a compact population in the pTP and another one with larger cells was located in the nTP. The posterior tubercle dopamine cells project primarily down into the brains stem and spinal cord (Tay et al., 2011), but some ascending projections to the telencephalon were also present (Rink and Wullimann, 2001). In this respect, they are similar to the A11 cell population of mammals (Björklund and Skagerberg, 1979; Takada et al., 1988; Takada, 1993). Traditionally, they are thought to modulate locomotion in the spinal cord, but there is accumulating evidence that descending projections also effect early sensory processing (Reinig et al., 2017; Haehnel-Taguchi et al., 2018). The nTP cells showed the largest activation in the Avoidance group and only weak activation in the Trained group. There was also some activation in the pTP. Individuals in the Avoidance group received very strong stimulation by being chased with a net, which enforced locomotion. But this also stimulated other senses with primary centers in the brain stem and spinal cord (lateral line, cutaneous mechanoreception, hearing/vestibular system). More refined experiments are necessary to discriminate between an activation of locomotion and the modulation of sensory processing.

4.1.6. Superior raphe

The superior raphe is known as a source of most of the serotonergic innervation within the brain. A subset of raphe cells are also known to produce dopamine in mammals (e.g. Ochi and Shimizu, 1978; Trulson et al., 1985; Stratford and Wirtshafter, 1990). It has been demonstrated that in mice their activity can be affected by learning (Groessl et al., 2018; Lin et al., 2020; Cho et al., 2021) and that are also involved in the formation and expression of aversive memory (Groessl et al., 2018; Lin et al., 2020), arousal and response to significant external events (Cho et al., 2017). Furthermore, the activity of dopaminergic neurons of the raphe reflects the incentive salience of the stimulus (Lin et al., 2021). In particular, dopaminergic neurons in the raphe are activated by rewarding stimuli, similar to the VTA neurons. Unlike these, raphe dopaminergic neurons are activated also by aversive stimuli (Matthews et al., 2016; Cho et al., 2017; Groessl et al., 2018). Therefore, experimental data show that raphe dopaminergic neurons encode the salience but not the valence of the stimuli (Lin et al., 2021). In fish, there are only two studies showing TH+ cells in the raphe (Ekström et al., 1990; Batten et al., 1993), but TH+ cells were consistently detected in the superior raphe in our material. The reason why other studies failed to detect TH+ cells in the raphe could be related to the observation that dopaminergic cells in the raphe respond to social isolation or the recovery from it (Matthews et al., 2016). They may have significant amounts of TH only under these conditions or they may have been overlooked since most studies focus on forebrain dopaminergic system in fish. Nevertheless, there was a strong activation of TH+ Ras cells in both the

Avoidance and Trained groups. Whether this is due to general arousal in these groups need to be determined with more refined experiments.

4.1.7. Locus coeruleus

Although the locus coeruleus is not dopaminergic, it is included in our study because it shows TH+ staining due to the production of another catecholamine, noradrenaline (Smeets and González, 2000). It shows 100% co-labeling with pS6 antibodies in the Isolation group, whereas the co-labeling was very low in other TH+ areas. In the Avoidance and Trained groups some non-double-labeled cells were found, but this was not significant. We don't know why the locus coeruleus shows a permanent activation in contrast to the dopaminergic cell populations. The locus coeruleus is interesting as it may play a role in attention and arousal (Ross and Van Bockstaele, 2021; Maness et al., 2022). However, it is unlikely that pS6 is modulating the arousal level because of the 100% labeling with pS6 in the Isolation group and the presence of pS6 in other larger neurons as well.

4.2. Multivariate analyses

Our multivariate analyses revealed complex co-activation patterns of dopaminergic and noradrenergic cell populations. Specifically, hierarchical clustering of the double-labeled TH+ cell populations demonstrated robust group differences in activity patterns. There is only one Trained specimen grouped together with the Avoidance cluster and one Isolation in the Trained cluster (see Fig. S1). PC1 of the PCA we conducted confirmed that differences between groups were largely driven by co-activation of a combination of the SCN, nTP, and superior raphe, suggesting that these activated TH+ cells might encode aspects of (negative) valence and possibly high salience associated with stressful stimuli of both the Avoidance stimulus and Trained task. Interestingly, double-labeled TH+ cells in the SCN and superior raphe loaded even more strongly on PC2, though in opposition to each other, thereby separating the Trained group from the other two experimental groups. This result may suggest that dopaminergic neurons in SCN and superior raphe may also have a learning and memory function in teleosts. Clearly, more detailed studies are required to understand these relationships better, and our results point at potentially profitable avenues of future research.

5. Conclusions

In the present study, we investigated the activation of dopaminergic cell populations by co-labeling TH and pS6 in individuals of the cichlid fish *P. zebra* subjected to different behavioral conditions. The dopaminergic system is composed of different subsystems with different functions ranging from sensory perception, hormonal control, regulating locomotion, to reward driven learning. The nature of each situation and any past experiences can change the balance of these subsystems and determine a complex emotional or motivational state of the animal. It is the first time the dopaminergic system has been investigated so in depth in a teleost, in particular showing how the activity of different dopaminergic cell populations are modulated in different behavioral conditions.

Ethical approval

The research reported herein was performed under the guidelines established by the EU Directive 2010/63/EU for animal experiments and the current German animal protection law and had been approved by the Landesamt für Natur, Umwelt und Verbraucherschutz NRW (approval number 8.87–50.10.37.09.198).

Funding

This work was funded by the Deutsche Forschungsgemeinschaft (SCHL 1919/5-1).

Author statement

Calvo and Schluessel contributed to the study conception and design. Data collection, processing of brains and sections were performed by Calvo under the supervision of Hofmann HA in Austin, Texas, US. Hofmann MH designed the data analysis procedure, and Calvo analyzed the data. The first draft of the manuscript was written by Calvo and all authors commented on previous versions of the manuscript. All authors read and approved the final manuscript.

Declaration of Competing Interest

The authors have no conflicts of interest to declare.

Acknowledgments

We thank the students Elaine Osterkamp, Andy Lam, and Ruben Eich for helping with the behavioral experiments. We also thank Jiawei Han for providing the R script. A special thanks also to the reviewers who invested an unusual amount of time and work to help improving the paper.

Appendix A. Supporting information

Supplementary data associated with this article can be found in the online version at doi:10.1016/j.jchemneu.2023.102342.

References

Anglade, I., Zandbergen, T., Kah, O., 1993. Origin of the pituitary innervation in the goldfish. Cell. Tissue Res. 273, 345–355.
Anthony, P.K., Stoltz, R.A., Pucci, M.L., Powers, C.A., 1993. The 22K variant of rat prolactin: evidence for identity to prolactin-(1-173), storage in secretory granules, and regulated release. Endocrinology 132, 806–814.
Antle, M.C., Mistlberger, R.E., 2000. Circadian clock resetting by sleep deprivation without exercise in the Syrian hamster. J. Neurosci. 20, 9326–9332.
de Arriba, Md.C., Pombal, M.A., 2007. Afferent connections of the optic tectum in lampreys: an experimental study. Brain Behav. Evol. 69, 37–68.
Batten, T., Berry, P., Maqbool, A., Moons, L., Vandesande, F., 1993. Immunolocalization of catecholamine enzymes, serotonin, dopamine and L-dopa in the brain of *Dicentrarchus labrax* (teleostei). Brain Res. Bull. 31, 233–252.
Ben-Jonathan, N., 1985. Dopamine: a prolactin-inhibiting hormone. Endocr. Rev. 6, 564–589.
Berridge, K.C., Robinson, T.E., 1998. What is the role of dopamine in reward: hedonic impact, reward learning, or incentive salience? Brain Res. Rev. 28, 309–369.
Bhat, S.K., Ganesh, C.B., 2020. Domperidone treatment attenuates stress-induced suppression of reproduction in viviparous mosquitofish *Gambusia affinis*. J. Fish. Biol. 96, 37–48.
Björklund, A., Skagerberg, G., 1979. Simultaneous use of retrograde fluorescent tracers and fluorescence histochemistry for convenient and precise mapping of monoaminergic projections and collateral arrangements in the CNS. J. Neurosci. Methods 1, 261–277.
Bolton, A.D., Murata, Y., Kirchner, R., Kim, S.-Y., Young, A., Dang, T., Yanagawa, Y., Constantine-Paton, M., 2015. A diencephalic dopamine source provides input to the superior colliculus, where D1 and D2 receptors segregate to distinct functional zones. Cell Rep. 13, 1003–1015.
Borgonovo, J., Ahumada-Galleguillos, P., Oñate-Ponce, A., Allende-Castro, C., Henny, P., Concha, M.L., 2021. Organization of the catecholaminergic system in the short-lived fish *Nothobranchius furzeri*. Front. Neuroanat. 15, 728720.
Callier, S., Snapyan, M., Le Crom, S., Prou, D., Vincent, J.D., Vernier, P., 2003. Evolution and cell biology of dopamine receptors in vertebrates. Biol. Cell. 95, 489–502.
Calvo, R., Schluessel, V., 2021. Neural substrates involved in the cognitive information processing in teleost fish. Anim. Cogn. 24, 923–946.
Calvo, R., Hofmann, M.H., Schluessel, V., 2023. Brain areas activated during visual learning in the cichlid fish *Pseudotropheus zebra*. Brain Struct. Funct. 228, 859–873.
Chabbi, A., Ganesh, C.B., 2015. Evidence for the involvement of dopamine in stress-induced suppression of reproduction in the cichlid fish *Oreochromis mossambicus*. J. Neuroendocrinol. 27, 343–356.
Cho, J.R., Treweek, J.B., Robinson, J.E., Xiao, C., Bremner, L.R., Greenbaum, A., Gradinaru, V., 2017. Dorsal raphe dopamine neurons modulate arousal and promote wakefulness by salient stimuli. Neuron 94, 1205–1219 e1208.
Cho, J.R., Chen, X., Kahan, A., Robinson, J.E., Wagenaar, D.A., Gradinaru, V., 2021. Dorsal raphe dopamine neurons signal motivational salience dependent on internal and external states. J. Neurosci. 24, 2645–2655.

Corio, M., Peute, J., Steinbusch, H., 1991. Distribution of serotonin-and dopamine-immunoreactivity in the brain of the teleost *Clarias gariepinus*. J. Chem. Neuroanat. 4, 79–95.
Dahlström, A., Fuxe, K., 1964. Localization of monoamines in the lower brain stem. Experientia 20, 398–399.
Demarest, K.T., Riegle, G.D., Moore, K.E., 1984. Prolactin-induced activation of tuberoinfundibular dopaminergic neurons: evidence for both a rapid 'tonic' and a delayed 'induction' component. Neuroendocrinology 38, 467–475.
Ekström, P., Honkanen, T., Steinbusch, H.W., 1990. Distribution of dopamine-immunoreactive neuronal perikarya and fibres in the brain of a teleost, *Gasterosteus aculeatus* L. comparison with tyrosine hydroxylase- and dopamine-beta-hydroxylase-immunoreactive neurons. J. Chem. Neuroanat. 3, 233–260.
El-Ghundi, M., O'Dowd, B.F., George, S.R., 2007. Insights into the role of dopamine receptor systems in learning and memory. Rev. Neurosci. 18, 37–66.
Enger, P.S., 1957. The electroencephalogram of the codfish (*Gadus callarias*); spontaneous electrical activity and reaction to photic and acoustic stimulation. Acta Physiol. Scand. 39, 55–72.
Fernstrom, J.D., Fernstrom, M.H., 2007. Tyrosine, phenylalanine, and catecholamine synthesis and function in the brain. J. Nutr. 137, 1539S–1547S.
Fiebig, E., Ebbesson, S., Meyer, D., 1983. Afferent connections of the optic tectum in the piranha (*Serrasalmus nattereri*). Cell Tissue Res 231, 55–72.
Filippi, A., Mahler, J., Schweitzer, J., Driever, W., 2010. Expression of the paralogous tyrosine hydroxylase encoding genes th1 and th2 reveals the full complement of dopaminergic and noradrenergic neurons in zebrafish larval and juvenile brain. J. Comp. Neurol. 518, 423–438.
Fontaine, R., Affaticati, P., Bureau, C., Colin, I., Demarque, M., Dufour, S., Vernier, P., Yamamoto, K., Pasqualini, C., 2015. Dopaminergic neurons controlling anterior pituitary functions: anatomy and ontogenesis in zebrafish. Endocrinology 156, 2934–2948.
Freeman, M.E., Kanyicska, B., Lerant, A., Nagy, G., 2000. Prolactin: structure, function, and regulation of secretion. Physiol. Rev. 80 (4), 1523–1631.
Goebrecht, G.K., Kowtoniuk, R.A., Kelly, B.G., Kittelberger, J.M., 2014. Sexually-dimorphic expression of tyrosine hydroxylase immunoreactivity in the brain of a vocal teleost fish (*Porichthys notatus*). J. Chem. Neuroanat. 56, 13–34.
Grippo, R.M., Tang, Q., Zhang, Q., Chadwick, S.R., Gao, Y., Altherr, E.B., Sipe, L., Purohit, A.M., Purohit, N.M., Sunkara, M.D., 2020. Dopamine signaling in the suprachiasmatic nucleus enables weight gain associated with hedonic feeding. Curr. Biol. 30, 196–208 e198.
Groessl, F., Munsch, T., Meis, S., Griessner, J., Kaczanowska, J., Pliota, P., Kargl, D., Badurek, S., Kraitsy, K., Rassoulpour, A., 2018. Dorsal tegmental dopamine neurons gate associative learning of fear. Nat. Neurosci. 21, 952–962.
Grover, B., Sharma, S., 1981. Organization of extrinsic tectal connections in goldfish (*Carassius auratus*). J. Comp. Neurol. 196, 471–488.
Haehnel-Taguchi, M., Fernandes, A.M., Böhler, M., Schmitt, I., Tittel, L., Driever, W., 2018. Projections of the diencephalospinal dopaminergic system to peripheral sense organs in larval zebrafish (*Danio rerio*). Front. Neuroanat. 12, 20.
Hikosaka, O., Nakamura, K., Sakai, K., Nakahara, H., 2002. Central mechanisms of motor skill learning. Curr. Opin. Neurobiol. 12, 217–222.
Hökfelt, T., 1984. Distributional maps of tyrosine-hydroxylase-immunoreactive neurons in the rat brain. Handb. Chem. Neuro. 2, 277–282.
Hornby, P.J., Piekut, D.T., Demski, L.S., 1987. Localization of immunoreactive tyrosine hydroxylase in the goldfish brain. J. Comp. Neurol. 261, 1–14.
Horvitz, J.C., 2000. Mesolimbocortical and nigrostriatal dopamine responses to salient non-reward events. Neuroscience 96, 651–656.
Ikemoto, S., Panksepp, J., 1999. The role of nucleus accumbens dopamine in motivated behavior: a unifying interpretation with special reference to reward-seeking. Brain Res. Rev. 31, 6–41.
Ito, H., Murakami, T., Fukuoka, T., Kishida, R., 1986. Thalamic fiber connections in a teleost (*Sebastiscus marmoratus*): visual somatosensory, octavolateral, and cerebellar relay region to the telencephalon. J. Comp. Neurol. 250, 215–227.
Kah, O., Chambolle, P., Thibault, J., Geffard, M., 1984. Existence of dopaminergic neurons in the preoptic region of the goldfish. Neurosci. Lett. 48, 293–298.
Kah, O., Dubourg, P., Onteniente, B., Geffard, M., Calas, A., 1986. The dopaminergic innervation of the goldfish pituitary. An immunocytochemical study at the electron-microscope level using antibodies against dopamine. Cell Tissue Res 244, 577–582.
Kah, O., Dulka, J.G., Dubourg, P., Thibault, J., Peter, R.E., 1987. Neuroanatomical substrate for the inhibition of gonadotrophin secretion in goldfish: existence of a dopaminergic preoptico-hypophyseal pathway. Neuroendocrinology 45, 451–458.
Kaslin, J., Panula, P., 2001. Comparative anatomy of the histaminergic and other aminergic systems in zebrafish (*Danio rerio*). J. Comp. Neurol. 440, 342–377.
Kelley, A.E., Berridge, K.C., 2002. The neuroscience of natural rewards: relevance to addictive drugs. J. Neurosci. 22, 3306–3311.
Kolde, R., 2012. Pheatmap: pretty heatmaps. R package version 1, 726.
Korshunov, K.S., Blakemore, L.J., Trombley, P.Q., 2017. Dopamine: a modulator of circadian rhythms in the central nervous system. Front. Cell. Neurosci. 11, 91.
Kress, S., Wullimann, M.F., 2012. Correlated basal expression of immediate early gene egr1 and tyrosine hydroxylase in zebrafish brain and downregulation in olfactory bulb after transitory olfactory deprivation. J. Chem. Neuroanat. 46, 51–66.
Kumar, S., Singh, U., Saha, S., Singru, P.S., 2014. Tyrosine Hydroxylase in the Olfactory System, Forebrain and Pituitary of the Indian Major Carp, *Cirrhinus cirrhosus*: Organisation and Interaction with Neuropeptide Y in the Preoptic Area. J. Neuroendocrinol. 26, 400–411.
Leard, L.E., Macdonald, E.S., Heller, H.C., Kilduff, T.S., 1994. Ontogeny of photic-induced c-fos mRNA expression in rat suprachiasmatic nuclei. Neuroreport 5, 2683–2687.
Lin, R., Liang, J., Wang, R., Yan, T., Zhou, Y., Liu, Y., Feng, Q., Sun, F., Li, Y., Li, A., Gong, H., Luo, M., 2020. The raphe dopamine system controls the expression of incentive memory. Neuron 106, 498–514 e498.
Lin, R., Liang, J., Luo, M., 2021. The raphe dopamine system: roles in salience encoding, memory expression, and addiction. Trends Neurosci. 44, 366–377.
Linard, B., Anglade, I., Corio, M., Navas, J.M., Pakdel, F., Saligaut, C., Kah, O., 1996. Estrogen receptors are expressed in a subset of tyrosine hydroxylase-positive neurons of the anterior preoptic region in the rainbow trout. Neuroendocrinology 63, 156–165.
Lindvall, O., Björklund, A., 1984. General organization of cortical monoamine systems. In: Descarries L, Reader TR, Jasper HH, editors. Monoamine innervation of the cerebral cortex. Liss; New York. pp. 9–40.
López-García, C., Molowny, A., Martínez Guijarro, F., Blasco-lbáñez, J., Luis de la Iglesia, J., Bernabeu, A., Garcia-Verdugo, J., 1992. Lesion and regeneration in the medical cerebral cortex of lizards. Histol. Histopathol.
Lowrey, P.L., Takahashi, J.S., 2011. Genetics of circadian rhythms in Mammalian model organisms. Adv. Genet. 74, 175–230.
Lu, Q., Kim, J.Y., 2022. Mammalian circadian networks mediated by the suprachiasmatic nucleus. FEBS J. 289, 6589–6604.
Luiten, P., 1981. Afferent and efferent connections of the optic tectum in the carp (*Cyprinus carpio L.*). Brain Res. 220, 51–65.
Ma, P.M., 1994. Catecholaminergic systems in the zebrafish. I. Number, morphology, and histochemical characteristics of neurons in the locus coeruleus. J. Comp. Neurol. 344, 242–255.
Macedo-Lima, M., Remage-Healey, L., 2021. Dopamine modulation of motor and sensory cortical plasticity among vertebrates. Integr. Comp. Biol. 61, 316–336.
Maness, E.B., Burk, J.A., McKenna, J.T., Schiffino, F.L., Strecker, R.E., McCoy, J.G., 2022. Role of the locus coeruleus and basal forebrain in arousal and attention. Brain Res. Bull. 1 (188), 47–58.
Manso, M.J., Becerra, M., Molist, P., Rodriguez-Moldes, I., Anadon, R., 1993. Distribution and development of catecholaminergic neurons in the brain of the brown trout. A tyrosine hydroxylase immunohistochemical study. J. Hirnforsch. 34, 239–260.
Matthews, G.A., Nieh, E.H., Vander Weele, C.M., Halbert, S.A., Pradhan, R.V., Yosafat, A. S., Glober, G.F., Izadmehr, E.M., Thomas, R.E., Lacy, G.D., 2016. Dorsal raphe dopamine neurons represent the experience of social isolation. Cell 164, 617–631.
Meek, J., Joosten, H., Hafmans, T., 1993. Distribution of noradrenaline-immunoreactivity in the brain of the mormyrid teleost *Gnathonemus petersii*. J. Comp. Neurol. 328, 145–160.
Mendoza, J., Challet, E., 2014. Circadian insights into dopamine mechanisms. Neuroscience 282, 230–242.
Meredith, G.E., Smeets, W.J., 1987. Immunocytochemical analysis of the dopamine system in the forebrain and midbrain of *Raja radiata*: evidence for a substantia nigra and ventral tegmental area in cartilaginous fish. J. Comp. Neurol. 265, 530–548.
Mistlberger, R.E., Antle, M.C., 2011. Entrainment of circadian clocks in mammals by arousal and food. Essays Biochem 49, 119–136.
Mistlberger, R.E., Skene, D.J., 2004. Social influences on mammalian circadian rhythms: animal and human studies. Biol. Rev. Camb. Philos. Soc. 79, 533–556.
Montardy, Q., Kwan, W.C., Mundinano, I.C., Fox, D.M., Wang, L., Gross, C.T., Bourne, J. A., 2021. Mapping the neural circuitry of predator fear in the nonhuman primate. Brain Struct. Funct. 226, 195–205.
Moore, H.A., Whitmore, D., 2014. Circadian rhythmicity and light sensitivity of the zebrafish brain. PloS One 9, e86176.
Moore, K.E., Demarest, K.T., Lookingland, K.J., 1987. Stress, prolactin and hypothalamic dopaminergic neurons. Neuropharmacology 26, 801–808.
Moroz, L.L., Romanova, D.Y., Kohn, A.B., 2021. Neural versus alternative integrative systems: molecular insights into origins of neurotransmitters. Philos. Trans. R. Soc. B 376 (1821), 20190762.
Naderi, M., Jamwal, A., Ferrari, M.C.O., Niyogi, S., Chivers, D.P., 2016. Dopamine receptors participate in acquisition and consolidation of latent learning of spatial information in zebrafish (*Danio rerio*). Prog. Neuropsychopharmacol. Biol. Psychiatry 67, 21–30.
Nagatsu, T., 2007. The catecholamine system in health and disease -Relation to tyrosine 3-monooxygenase and other catecholamine-synthesizing enzymes. Proc. Jpn. Acad. Ser. B. Phys. Biol. Sci. 82, 388–415.
O'Connell, L.A., Hofmann, H.A., 2011. Genes, hormones, and circuits: an integrative approach to study the evolution of social behavior. Front. Neuroendocr. 32 (3), 320–335.
Ochi, J., Shimizu, K., 1978. Occurrence of dopamine-containing neurons in the midbrain raphe nuclei of the rat. Neurosci. Lett. 8, 317–320.
O'Connell, L., Rigney, M., Dykstra, D., Hofmann, H., 2013b. Neuroendocrine mechanisms underlying sensory integration of social signals. J. Neuroendocrinol. 25.
O'Connell, L.A., Fontenot, M.R., Hofmann, H.A., 2011. Characterization of the dopaminergic system in the brain of an African cichlid fish, *Astatotilapia burtoni*. J. Comp. Neurol. 519, 75–92.
O'Connell, L.A., Fontenot, M.R., Hofmann, H.A., 2013a. Neurochemical profiling of dopaminergic neurons in the forebrain of a cichlid fish, *Astatotilapia burtoni*. J. Chem. Neuroanat. 47, 106–115.
Parafati, M., Senatori, O., Nicotra, A., 2009. Localization of tyrosine hydroxylase immunoreactive neurons in the forebrain of the guppy *Poecilia reticulata*. J. Fish. Biol. 75, 1194–1205.
Perez-Perez, M.P., Luque, M.A., Herrero, L., Nunez-Abades, P.A., Torres, B., 2003. Afferent connectivity to different functional zones of the optic tectum in goldfish. Vis. Neurosci. 20 (4), 397–410.
Pierre, J., Mahouche, M., Suderevskaya, E.I., Repérant, J., Ward, R., 1997. Immunocytochemical localization of dopamine and its synthetic enzymes in the

central nervous system of the lamprey *Lampetra fluviatilis*. J. Comp. Neurol. 380 (1), 119–135.
Piña-Leyva, C., Lara-Lozano, M., Rodríguez-Sánchez, M., Vidal-Cantú, G.C., Barrientos Zavalza, E., Jiménez-Estrada, I., Delgado-Lezama, R., Rodríguez-Sosa, L., Granados-Soto, V., González-Barrios, J.A., Florán-Garduño, B., 2022. Hypothalamic A11 nuclei regulate the circadian rhythm of spinal mechanonociception through dopamine receptors and clock gene expression. Life 12, 1411.
Piñuela, C., Northcutt, R.G., 2007. Immunohistochemical organization of the forebrain in the white sturgeon, *Acipenser transmontanus*. Brain Behav. Evol. 69, 229–253.
Pollen, A.A., Dobberfuhl, A.P., Scace, J., Igulu, M.M., Renn, S.C.P., Shumway, C.A., Hofmann, H.A., 2007. Environmental complexity and social organization sculpt the brain in lake tanganyikan cichlid fish. Brain Behav. Evol. 70, 21–39.
Pombal, M.A., Manira, A.E., Grillner, S., 1997. Afferents of the lamprey striatum with special reference to the dopaminergic system: a combined tracing and immunohistochemical study. J. Comp. Neurol. 386 (1), 71–91.
Puig, M.V., Rose, J., Schmidt, R., Freund, N., 2014. Dopamine modulation of learning and memory in the prefrontal cortex: insights from studies in primates, rodents, and birds. Front. Neural Circuits 5 8, 93.
Pushchina, E., 2009. Tyrosine hydroxylase in telencephalon and diencephalon of *Rhodeus sericeus* (Cyprinidae). Tsitologiia 51, 63–77.
Qu, S., Ondo, W.G., Zhang, X., Xie, W.J., Pan, T.H., Le, W.D., 2006. Projections of diencephalic dopamine neurons into the spinal cord in mice. Exp. Brain Res. 168, 152–156.
Reiner, A., Northcutt, R.G., 1987. An immunohistochemical study of the telencephalon of the African lungfish, *Protopterus annectens*. J. Comp. Neurol. 256, 463–481.
Reinig, S., Driever, W., Arrenberg, A.B., 2017. The descending diencephalic dopamine system is tuned to sensory stimuli. Curr. Biol. 27, 318–333.
Reppert, S.M., Weaver, D.R., 2002. Coordination of circadian timing in mammals. Nature 418, 935–941.
Rink, E., Wullimann, M.F., 2001. The teleostean (zebrafish) dopaminergic system ascending to the subpallium (striatum) is located in the basal diencephalon (posterior tuberculum). Brain Res. 889, 316–330.
Roberts, B.L., Meredith, G.E., Maslam, S., 1989. Immunocytochemical analysis of the dopamine system in the brain and spinal cord of the European eel, *Anguilla anguilla*. Anat. Embryol. 180, 401–412.
Rodman, H.R., Karten, H.J., 1995. Laminar distribution and sources of catecholaminergic input to the optic tectum of the pigeon (*Columba livia*). J. Comp. Neurol. 359, 424–442.
Rodríguez-Gómez, F., Rendón-Unceta, M., Sarasquete, C., Munoz-Cueto, J., 2000. Localization of tyrosine hydroxylase-immunoreactivity in the brain of the Senegalese sole, *Solea senegalensis*. J. Chem. Neuroanat. 19, 17–32.
Ross, J.A., Van Bockstaele, E.J., 2021. The locus coeruleus-norepinephrine system in stress and arousal: unraveling historical, current, and future perspectives. Front. Psychiatry 11, 601519.
Salamone, J.D., Cousins, M.S., Snyder, B.J., 1997. Behavioral functions of nucleus accumbens dopamine: empirical and conceptual problems with the anhedonia hypothesis. Neurosci. Biobehav. Rev. 21, 341–359.
Sánchez-Vázquez, F., Madrid, J., Zamora, S., Tabata, M., 1997. Feeding entrainment of locomotor activity rhythms in the goldfish is mediated by a feeding-entrainable circadian oscillator. J. Comp. Physiol. A 181, 121–132.
Sas, E., Maler, L., Tinner, B., 1990. Catecholaminergic systems in the brain of a gymnotiform teleost fish: an immunohistochemical study. J. Comp. Neurol. 292, 127–162.
Schluessel, V., Hiller, J., Krueger, M., 2018. Discrimination of movement and visual transfer abilities in cichlids (*Pseudotropheus zebra*). Behav. Ecol. Sociobiol. 72, 61.
Schlussman, S., Kobylack, M., Dunn-Meynell, A., Sharma, S., 1990. Afferent connections of the optic tectum in channel catfish *Ictalurus punctatus*. Cell Tissue Res 262, 531–541.
Semenova, S.A., Chen, Y.C., Zhao, X., Rauvala, H., Panula, P., 2014. The tyrosine hydroxylase 2 (TH2) system in zebrafish brain and stress activation of hypothalamic cells. Histochem. Cell. Biol. 142, 619–633.
Shin, S.H., 1979. Prolactin secretion in acute stress is controlled by prolactin releasing factor. Life Sci. 25, 1829–1835.
Shumway, C.A., 2008. Habitat complexity, brain, and behavior. Brain Behav. Evol. 72, 123–134.
Shumway, C.A., 2010. The evolution of complex brains and behaviors in African cichlid fishes. Curr. Zool. 56, 144–156.
Smeets, W.J., González, A., 2000. Catecholamine systems in the brain of vertebrates: new perspectives through a comparative approach. Brain Res. Rev. 33, 308–379.
Smeets, W.J., Hoogland, P.V., Voorn, P., 1986. The distribution of dopamine immunoreactivity in the forebrain and midbrain of the lizard *Gekko gecko*: an immunohistochemical study with antibodies against dopamine. J. Comp. Neurol. 253, 46–60.
Stratford, T.R., Wirtshafter, D., 1990. Ascending dopaminergic projections from the dorsal raphe nucleus in the rat. Brain Res 511, 173–176.
Striedter, G.F., 1990. The diencephalon of the channel catfish, *Ictalurus punctatus*. Brain Behav. Evol. 36, 355–377.
Sunuma, T., Amano, M., Iigo, M., Yamamori, K., 2009. Food-entrainable circadian oscillator in goldfish: multiple daily feeding times and food-anticipatory activity. Fish. Sci. 75, 207–214.
Suzuki, R., Shimodaira, H., 2006. Pvclust: an R package for assessing the uncertainty in hierarchical clustering. Bioinform 22, 1540–1542.
Tahara, Y., Shibata, S., 2018. Entrainment of the mouse circadian clock: effects of stress, exercise, and nutrition. Free Radic. Biol. Med. 119, 129–138.
Takada, M., 1993. Widespread dopaminergic projections of the subparafascicular thalamic nucleus in the rat. Brain Res. Bull. 32, 301–309.
Takada, M., Li, Z., Hattori, T., 1988. Single thalamic dopaminergic neurons project to both the neocortex and spinal cord. Brain Res 455, 346–352.
Takakuwa, N., Kato, R., Redgrave, P., Isa, T., 2017. Emergence of visually-evoked reward expectation signals in dopamine neurons via the superior colliculus in V1 lesioned monkeys. Elife 6, e24459.
Takeuchi, Y., Takashima, M., Katoh, Y., Nishikawa, T., Takahashi, K., 1991. N-Methyl-d-aspartate, quisqualate and kainate receptors are all involved in transmission of photic stimulation in the suprachiasmatic nucleus in rats. Brain Res 563, 127–131.
Tay, T.L., Ronneberger, O., Ryu, S., Nitschke, R., Driever, W., 2011. Comprehensive catecholaminergic projectome analysis reveals single-neuron integration of zebrafish ascending and descending dopaminergic systems. Nat. Commun. 2, 171.
Torner, L., 2016. Actions of prolactin in the brain: from physiological adaptations to stress and neurogenesis to psychopathology. Front. Endocrinol. 7, 25.
Trulson, M.E., Cannon, M.S., Raese, J.D., 1985. Identification of dopamine-containing cell bodies in the dorsal and median raphe nuclei of the rat brain using tyrosine hydroxylase immunochemistry. Brain Res. Bull. 15, 229–234.
Tuomisto, J., Männistö, P., 1985. Neurotransmitter regulation of anterior pituitary hormones. Pharmacol. Rev. 37, 249–332.
Valdés-Baizabal, C., Carbajal, G.V., Pérez-González, D., Malmierca, M.S., 2020. Dopamine modulates subcortical responses to surprising sounds. PLoS Biol. 18, e3000744.
Weitekamp, C., Hofmann, H., 2017. Neuromolecular correlates of cooperation and conflict during territory defense in a cichlid fish. Horm. Behav. 89.
Weltzien, F.A., Pasqualini, C., Sébert, M.E., Vidal, B., Le Belle, N., Kah, O., Vernier, P., Dufour, S., 2006. Androgen-dependent stimulation of brain dopaminergic systems in the female European eel (*Anguilla anguilla*). Endocrinology 147, 2964–2973.
Wintle, R.F., Van Tol, H.H.M., 2001. Dopamine signaling in Caenorhabditis elegans; potential for parkinsonism research. Park. Relat. Disord. 7, 177–183.
Wise, R.A., 2009. Roles for nigrostriatal–not just mesocorticolimbic–dopamine in reward and addiction. Trends Neurosci. 32, 517–524.
Yamamoto, K., Vernier, P., 2011. The evolution of dopamine systems in chordates. Front. Neuroanat. 5, 21.